



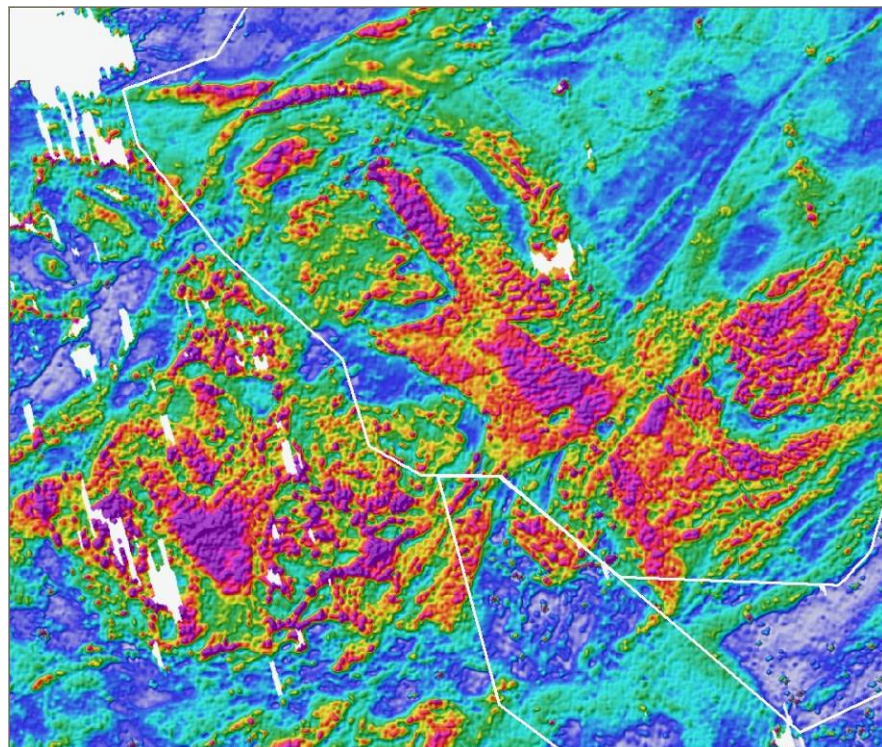
**British  
Geological Survey**

NATURAL ENVIRONMENT RESEARCH COUNCIL

# The construction of a merged EM (conductivity) database using Tellus and Tellus Border airborne geophysical data

Land Use, Planning and Development Programme

British Geological Survey Report OR/13/003





BRITISH GEOLOGICAL SURVEY

Land Use, Planning and Development Programme

OPEN REPORT OR/13/003

**The construction of a merged EM (conductivity) database using Tellus and Tellus Border airborne geophysical data**

The National Grid and other Ordnance Survey data are used with the permission of the Controller of Her Majesty's Stationery Office.  
Licence No: 100017897/2010.

David Beamish

*Keywords*

Report; Tellus, airborne survey, geophysics, electrical conductivity, geology

*Front cover*

Image of merged estimates of conductivity across 3 cross-border survey areas

*Bibliographical reference*

BEAMISH, D., 2013. *The construction of a merged EM (conductivity) database using Tellus and Tellus Border airborne geophysical data.* British Geological Survey Open Report, OR/13/003. 33pp.

Copyright in materials derived from the British Geological Survey's work is owned by the Natural Environment Research Council (NERC) and/or the authority that commissioned the work. You may not copy or adapt this publication without first obtaining permission. Contact the BGS Intellectual Property Rights Section, British Geological Survey, Keyworth, e-mail [ipr@bgs.ac.uk](mailto:ipr@bgs.ac.uk). You may quote extracts of a reasonable length without prior permission, provided a full acknowledgement is given of the source of the extract.

Maps and diagrams in this book use topography based on Ordnance Survey mapping.

© NERC 2013. All rights reserved

Keyworth, Nottingham British Geological Survey 2013



## BRITISH GEOLOGICAL SURVEY

The full range of our publications is available from BGS shops at Nottingham, Edinburgh, London and Cardiff (Welsh publications only) see contact details below or shop online at [www.geologyshop.com](http://www.geologyshop.com)

The London Information Office also maintains a reference collection of BGS publications, including maps, for consultation.

We publish an annual catalogue of our maps and other publications; this catalogue is available online or from any of the BGS shops.

*The British Geological Survey carries out the geological survey of Great Britain and Northern Ireland (the latter as an agency service for the government of Northern Ireland), and of the surrounding continental shelf, as well as basic research projects. It also undertakes programmes of technical aid in geology in developing countries.*

*The British Geological Survey is a component body of the Natural Environment Research Council.*

*British Geological Survey offices*

### **BGS Central Enquiries Desk**

Tel 0115 936 3143 Fax 0115 936 3276  
email [enquiries@bgs.ac.uk](mailto:enquiries@bgs.ac.uk)

### **Kingsley Dunham Centre, Keyworth, Nottingham NG12 5GG**

Tel 0115 936 3241 Fax 0115 936 3488  
email [sales@bgs.ac.uk](mailto:sales@bgs.ac.uk)

### **Murchison House, West Mains Road, Edinburgh EH9 3LA**

Tel 0131 667 1000 Fax 0131 668 2683  
email [scotsales@bgs.ac.uk](mailto:scotsales@bgs.ac.uk)

### **Natural History Museum, Cromwell Road, London SW7 5BD**

Tel 020 7589 4090 Fax 020 7584 8270  
Tel 020 7942 5344/45 email [bgs\\_london@bgs.ac.uk](mailto:bgs_london@bgs.ac.uk)

### **Columbus House, Greenmeadow Springs, Tongwynlais, Cardiff CF15 7NE**

Tel 029 2052 1962 Fax 029 2052 1963

### **Maclean Building, Crowmarsh Gifford, Wallingford OX10 8BB**

Tel 01491 838800 Fax 01491 692345

### **Geological Survey of Northern Ireland, Colby House, Stranmillis Court, Belfast BT9 5BF**

Tel 028 9038 8462 Fax 028 9038 8461

[www.bgs.ac.uk/gsni/](http://www.bgs.ac.uk/gsni/)

### *Parent Body*

### **Natural Environment Research Council, Polaris House, North Star Avenue, Swindon SN2 1EU**

Tel 01793 411500 Fax 01793 411501  
[www.nerc.ac.uk](http://www.nerc.ac.uk)

Website [www.bgs.ac.uk](http://www.bgs.ac.uk)

Shop online at [www.geologyshop.com](http://www.geologyshop.com)

# Foreword

This report is the published product of a study by the British Geological Survey (BGS) as part of the Land Use, Planning and Development Programme. The report provides a description of the work carried out under the provision of scientific services to the Tellus Border Project. The Tellus Border Project is a cross-border geo-environmental mapping project of Northern Ireland and the northern counties of the Republic of Ireland. The project is led by the Geological Survey of Northern Ireland (GSNI) in partnership with the Geological Survey of Ireland (GSI) and is financed by the INTERREG IVA programme of the European Regional Development Fund. The Tellus Border project extends the geophysical mapping of Northern Ireland previously undertaken by GSNI under the Tellus Project.

# Contents

<b>Foreword</b> .....	<b>i</b>
<b>Contents</b> .....	<b>i</b>
<b>1 Introduction</b> .....	<b>1</b>
<b>2 Technical Background</b> .....	<b>3</b>
2.1 Data Sets.....	3
2.2 Half-space conductivity transforms.....	4
2.3 Half space conductivity inversion.....	5
<b>3 Example application to the TEL-06 survey data</b> .....	<b>6</b>
3.1 Data levelling.....	12
<b>4 The Cavan Survey</b> .....	<b>15</b>
<b>5 The Tellus Border Survey</b> .....	<b>17</b>
5.1 Inversion of TB data.....	19
<b>6 Merging the 4 data sets (grids)</b> .....	<b>22</b>
6.1 Merging TEL-05 and TEL-06.....	22
6.2 Merging CAV and TB.....	23
6.3 Merging TEL-05-06 and CAVTB.....	24
<b>7 The merged conductivity database</b> .....	<b>25</b>
<b>8 References</b> .....	<b>27</b>
<b>Appendix 1</b> .....	<b>29</b>

## FIGURES

Figure 1. Outline polygons of the 3 surveys considered here. Tellus (TEL-05, TEL-06), Cavan (+Monaghan) CAV-06 and Tellus Border (TB-11-12). The polygon labelled C refers to the Conroy survey area reflown by TB-11-12..... 2

Figure 2. Survey outlines on base map of 1:500k bedrock geology and county outlines. Green zone is the commercial OST survey. ....	3
Figure 3. Levelled P,Q coupling ratios below the low value threshold limits for the TB data. (a) 0.9 kHz and (b) 12 kHz. ....	4
Figure 4. L1 misfit errors for the TEL-06 LF data. Blue areas denote urban zones. (a) Errors>25%. (b) Errors > 100%. ....	6
Figure 5. L1 misfit errors for the TEL-06 HF data. Blue areas denote urban zones. (a) Errors>25%. (b) Errors > 100%. ....	7
Figure 6. Detailed view of the L1 misfit errors > 100% for the TEL-06 LF data.....	7
Figure 7. Detailed view centered on 1x1 km square (in red) of the area of the Ballymacvea landfill. Existing LF apparent conductivity shown in a 5-band colour and proportional size scheme. The highest conductivities (> 80 mS/m) are shown in red. Black symbols denote the L1 misfit > 100% zones and partially track a power-line route. ....	8
Figure 8. Variation of L1 misfit error (clipped to 500%) and radar altitude (RALT) for the TEL-06 LF data set. ....	9
Figure 9. Variation of L1 misfit error (clipped to 500%) and radar altitude (RALT) for the TEL-06 HF data set. ....	10
Figure 10. Plot of transform and inversion apparent resistivity estimates for the TEL—06 LF data.....	11
Figure 11. Inversion result grids (detailed area) from the TEL-06 LF data. Both images use 50 m cells and equal-area colour. (a) Minimum-curvature grid. (b) Natural-neighbour grid. ....	12
Figure 12. Posted value plots of the FMD levelling corrections applied to the apparent resistivity model estimates for the TEL-06 data. Rotated (N-S) reference frame. (a) LF data. (b) HF data.....	13
Figure 13. Detailed area inversion result grids (NN) from the TEL-06 LF data. Both images use 50 m cells and equal-area colour. (a) Pre-levelled data. (b) FMD levelled data. ....	14
Figure 14. Transform (a) and inversion (b) shaded relief images of LF apparent conductivity across an area in the SW of the Tellus survey. Light source is +45° from north in both cases. E refers to Enniskillen. (a) Shows towns as infilled (yellow) polygons. (b) Shows high-fly zones > 175 m, as blanks. The central NE-SW structure is the Tempo-Sixmilecross Fault (TSF).....	15
Figure 15. L1 misfit errors (ERR) for the CAV (a) LF and (b) HF data. Lower image (b) also shows RALT>180 m. ....	16
Figure 16. Final apparent conductivity estimates for the CAV survey at (a) LF and (b) HF. The lower image is shown as a perspective view to indicate the dynamic range of both geological (spatially sustained) and non-geological (localised) influences in the processed data set. ....	17
Figure 17. (a) TB LF apparent conductivity. (B) Difference LF apparent conductivity TB minus CONROY. ....	18
Figure 18. (a) TB HF apparent conductivity. (B) Difference HF apparent conductivity TB minus CONROY. ....	19
Figure 19. Variation of L1 misfit error (clipped to 500%) and radar altitude (RALT) for the TB data set Lines L1000 to L13000. (a) LF and (b) HF.....	20
Figure 20. (a) Observed L1 misfit errors for the TB LF western data (5-100% in black, 100 to 500% in red). (b) RALT for the TB western data (120 to 180m in black, 180 to 791m in red).21	

Figure 21. (a) Observed L1 misfit errors for the TB HF eastern data (values>100%). (b) RALT for the TB eastern data (Values>180m). ..... 21

Figure 22. Transform (a) and inversion (b) images of TEL-05 LF apparent conductivity across an area centred on Milligan Point. (a) Shows towns as infilled (yellow) polygons. (b) Shows high-fly zones > 175 m, as blanks (white areas). Images are cut to coast..... 23

Figure 23. LF merged conductivity grid imaged using a linear colour scale (2 to 50 mS/m) with condition RALT>`175m defined by white zones. White lines denote survey boundaries. Black area denotes OST survey..... 24

Figure 24. HF merged conductivity grid imaged using a linear colour scale (2 to 50 mS/m) with condition RALT>`175m defined by white zones. White lines denote survey boundaries. Black area denotes OST survey..... 25

Figure 25. LF merged conductivity grid imaged using a linear colour scale (2 to 50 mS/m) with condition RALT>`175m defined by white zones and all data cut-to coast. Black area denotes OST survey..... 26

Figure A27. Comparison of sampling in altitude and resistivity of TransAEM and TransAEM07.30

Figure A28. TransAEM nomograms (digital look-up tables). ..... 30

Figure A29. TransAEM07 nomograms (digital look-up tables). ..... 31

# 1 Introduction

The airborne geophysical survey data sets considered here are the Northern Ireland (NI) Tellus (2005) and Tellus (2006) surveys (for the Geological Survey of Northern Ireland, GSNI), the Cavan (Cavan-Monaghan, 2006) survey (for the Geological Survey of Ireland, GSI) and the more recent Tellus Border survey (for GSI/GSNI). General information about the airborne and associated geochemical surveys can be found through links on the web pages at: <http://www.bgs.ac.uk/gsni/tellus/> and <http://www.tellusborder.eu/>

The airborne EM (AEM) data were all acquired using the same/similar electromagnetic (EM) system on board a De Havilland Twin-Otter aircraft. The EM system is fully described by Leväniemi, et al. (2009). Flight line orientation was 345° relative to geographic north, in all the surveys considered here. Again in all the surveys, a nominal survey height of about 180' (56 m) was subject to high-fly zones in relation to ground structures that were prescribed by the permitting procedure and by the clients. In broad terms, high-fly zones extending to 200 m and above, are associated with all conurbations of any significant size. Information on the 4 electromagnetic surveys, and additional commercial surveys (using the same EM system) is summarised in Table 1 and Figure 1.

**Table 1.** Summary of AEM geophysical survey data (2005-2012) considered here. NF refers to the number of frequencies used. The 2 frequency survey acquired data at 3125 and 14368 Hz. The 4 frequency surveys used 912, 3005, 11962 and 24510 Hz. JAC refers to the Joint Airborne-geoscience Capability operated by the Geological Survey of Finland and the British Geological Survey until 2009.

Survey	Year	Code	Airborne Contractor	NF	Sampling (Hz)
Tellus	2005	TEL-05	JAC	2	4
Tellus	2006	TEL-06	JAC	4	4
Cavan	2006	CAV	JAC	4	4
Tellus Border	2011-2012	TB	Sander	4	10
Commercial					
Conroy Diamonds and Gold plc	2006	CON	JAC	4	4
Oriel Selection Trust	2012	OST	Sander	4	10

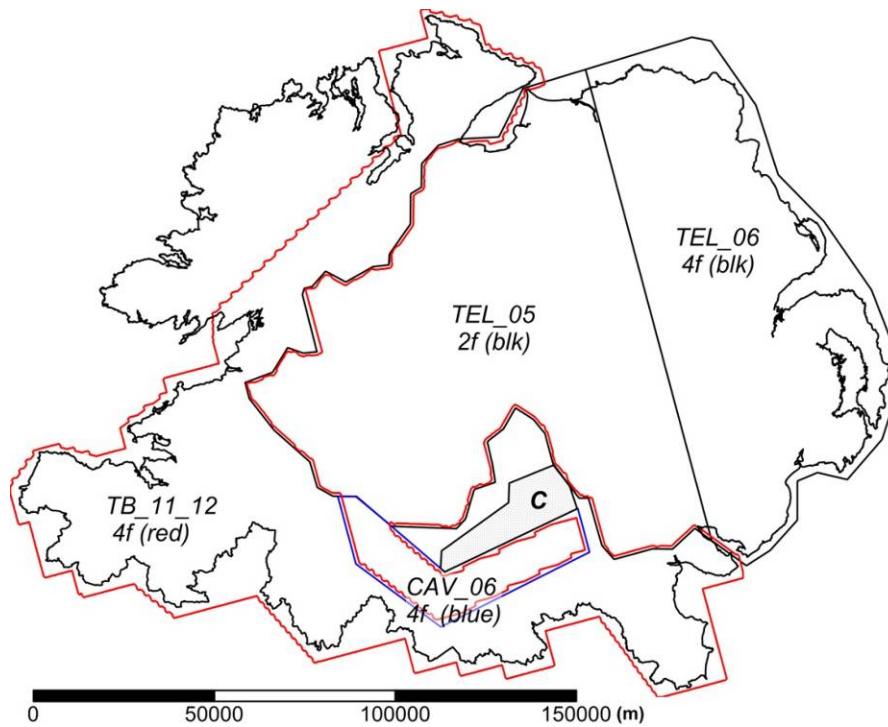


**Figure 1.** Outline polygons of the 3 surveys considered here. Tellus (TEL-05, TEL-06), Cavan (+Monaghan) CAV-06 and Tellus Border (TB-11-12). The polygon labelled C refers to the Conroy survey area reflowed by TB-11-12.

The two Tellus surveys, TEL-05 and TEL-06 extend ~1 to 2 km into the Republic of Ireland (ROI) and over the coastal zone of NI. The CAV survey provides no overlap with the Tellus surveys. The TB survey contains a zone of no-fly that corresponds to the CAV survey. The TB survey was designed to provide overlap zones with both the Tellus and CAV survey zones. The area labelled C corresponds to a commercial survey (Conroy) that was reflowed by the TB survey. The data were acquired (by JAC) in 2006 as an extended component of the CAV survey. The availability of the Conroy data, for research purposes, allows for data comparisons using the more recently acquired TB data sets. The survey polygons are shown on 1:500k bedrock geology map with county outlines. The commercial OST survey, an extension to the main TB survey, is identified in green. Figure 2 also identifies the coastal zones included in the Tellus and TB survey areas.

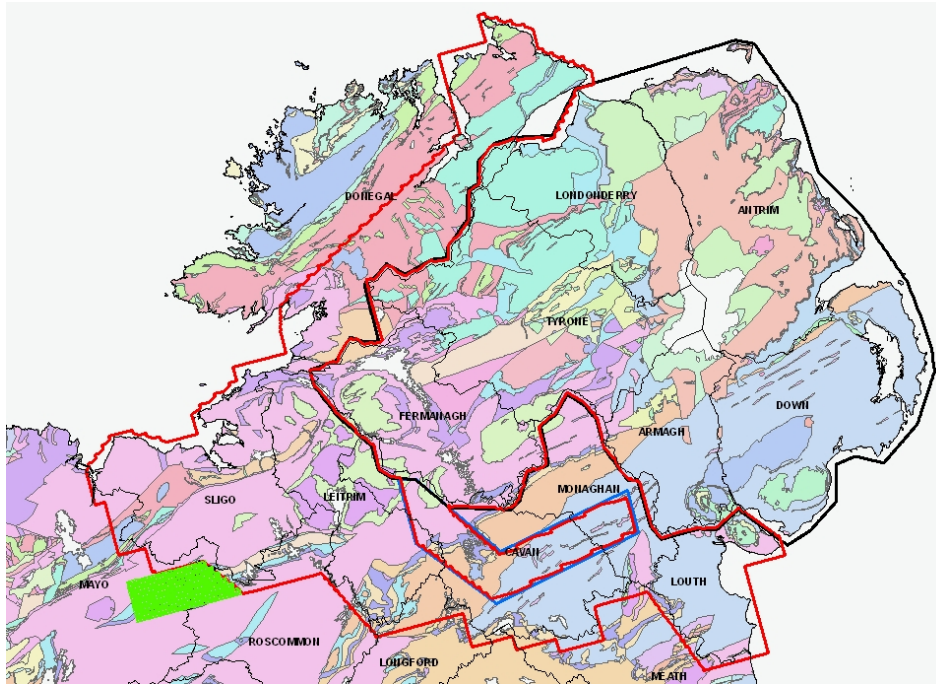


**Figure 2.** Survey outlines on base map of 1:500k bedrock geology and county outlines. Green zone is the commercial OST survey.

The scope of the present study is to provide merged conductivity estimates for the survey data discussed above. This is undertaken using specific (half-space) conductivity estimates obtained at individual frequencies from the primary EM data (coupling ratios). No attempt is made here to consider the calibration and multi-frequency validity of these estimates.

## 2 Technical Background

### 2.1 DATA SETS

The EM data used here are from contractor supplied final data files available through GSNI and GSI. Processing reports that accompany the data are also available from the 2 organisations. In EM data terms, the change from a 2 frequency system used in 2005 to a 4 frequency system used in 2006 (and thereafter) provides an added complication to merging the 4 primary data sets. The method used previously is described in the final processing report (Beamish et al., 2006; <http://nora.nerc.ac.uk/7427/1/IR06136.pdf>). EM data from two common frequencies (3125/3005 Hz) and (14,368/11,962 Hz) were used to construct low frequency (LF, 3125/3005 Hz) and high frequency (HF, 14,368/11,962 Hz) estimates of the half-space apparent conductivities/resistivities uniformly across the combined survey area. The procedures used also supplied uniform/merged estimates of the coupling ratios at each frequency. This was made possible by 2 control lines (LINES 1214 and 1215) repeated by both the 2005 and 2006 surveys and passing over the large water body of Lough Neagh. The use of a large body of water ensured that flying altitudes of the two control survey lines were well-maintained.

The primary EM survey data comprise complex coupling ratios referred to as P (real or in-phase, in ppm) and Q (imaginary or in-quadrature, in ppm) at each frequency. These data, along with altitude (ALT), may then be used to construct a half-space conductivity model. The P, Q data display a high degree of sensitivity to altitude (Beamish, 2002a,b; Beamish and Leväniemi, 2010) and unless identical altitudes are maintained in overlap zones between surveys, the ability to merge P,Q,ALT data is compromised.

The apparent conductivity data obtained by transform modelling of the P,Q data has no dependence on altitude and so these data can be simply merged across surveys. Although it is possible to consider merging conductivity models for the four frequency sets provided across 3 of the surveys, this procedure would, necessarily, omit the large and central area of the TEL-05 survey. In the first instance the production of merged conductivity data sets for all 4 surveys is undertaken at low frequency (LF, referred to as 3 kHz) and at high frequency (HF, referred to as 12-14 kHz).

## 2.2 HALF-SPACE CONDUCTIVITY TRANSFORMS

The apparent conductivity, or resistivity, data supplied by the contractors are generated by modern adaptations of a simple transform procedure (Fraser, 1978) that uses the P,Q data at each frequency but not the altitude. The transform also returns an apparent depth (AD) parameter (see Beamish, 2002a). A detailed, previously unpublished description of the transform procedure used by the JAC is included in Appendix 1. A similar procedure has been used to deliver apparent conductivities in the TB survey data.

Each specific AEM system has a limited conductivity aperture defined by system parameters and the signal/noise of the P,Q data acquired and processed. These are discussed in Appendix 1. In order to provide a valid estimate of apparent conductivity, each P,Q measurement must be greater than zero and also greater than the noise level of the measurement. Since different assignments of low value threshold values may be used in the processing of different survey data, the ability to merge different data sets across areas having low resistivity (say  $> 1,000$  ohm.m) may not be accurate.

Following the discussion in Appendix 1, we here set a low value threshold of P,Q = 20 ppm for low frequency data (0.9 and 3 kHz) and P,Q = 30 ppm for higher frequency data (12-14 and 25 kHz). These are estimates of the typical ‘best’ accuracy that can be achieved in the processing of the acquired P,Q coupling ratios. As an example, Figure 3 shows the P,Q values at and below the threshold values for the delivered (levelled) TB data at low frequency (0.9 kHz) and at higher frequency (12 kHz).

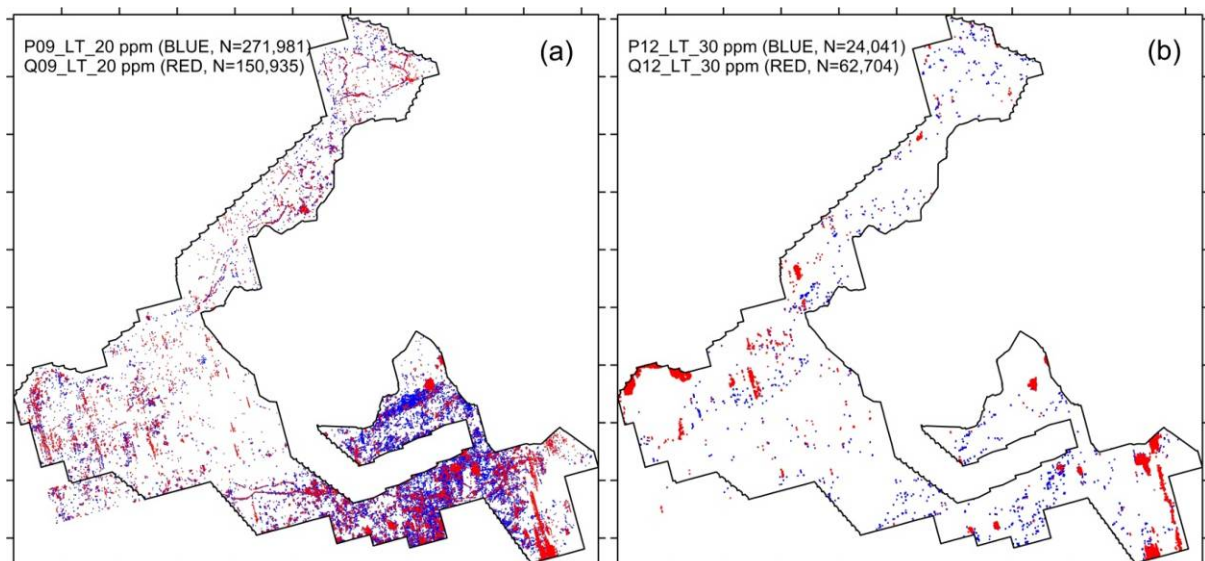


**Figure 3.** Levelled P,Q coupling ratios below the low value threshold limits for the TB data. (a) 0.9 kHz and (b) 12 kHz.

As is clearly demonstrated, the numbers below the threshold limit typically increase with decreasing frequency. In practice all the data points shown are defined as inadequate and are simply set to the artificial threshold of  $P,Q = 20$  ppm or  $P,Q = 30$  ppm. This aspect of the data behaviour and processing control is often overlooked when examining final images of half-space conductivities.

The transform procedure, while reliable, provides conservative estimates of apparent conductivity using a digital look-up algorithm (Appendix 1 and Beamish, 2002b). An alternative inversion procedure, used to model the P,Q,ALT data supplied by the contractors is now described

### 2.3 HALF SPACE CONDUCTIVITY INVERSION

The non-linear, least-squares half-space inversion described by Beamish (2002a) is used here. The inversion uses the P,Q,ALT data at each frequency and considers a model of a thin-resistive zone above a uniform half-space. The resistivity of the at-surface layer is fixed at 100,000 ohm.m but the thickness is allowed to vary. The ability of the thickness parameter (THK) to accommodate incorrect (underestimated) radar altimeter data due to canopy effects was demonstrated by Beamish (2002b). The second parameter returned by the inversion is the conductivity of the half-space. The inversion minimises the difference between the observed data (P,Q) and the response of the model. The result is a 'best-fitting' model with an error estimate describing how well the response of the model has been fitted to the observed data.

Due to the small numbers of observations used in the inversion (i.e. 2), an L1 norm (based on the sum of differences) rather than an L2 norm (based on the sum of squared differences) misfit parameter is used. Here the L1 norm percentage error is defined as:

$$L1 (\%) = 100 \sum_i | O_i - C_i | / C_i \quad \dots(1)$$

where the summation index (i) extends from 1 (P) to 2(Q).  $O_i$  is the i'th observation (an in-phase or in-quadrature coupling ratio) and  $C_i$  is the corresponding calculated value. L1 norms are typically greater than L2 norms (e.g. an rms misfit) by a factor of 10. This definition of misfit is used throughout. The L1 misfit term is referred to as the ERR (error) parameter of the inversion.

The error term is particularly useful since it allows inconsistent half-space conductivity model estimates to be rejected. Subsequent to the inversion, an estimate of centroid depth i.e. the mean depth of the induced in-phase current can also be provided. Following Siemon (2001), who used estimated apparent resistivity and apparent depth (AD), we here would calculate the centroid depth ( $C_d$ ) as

$$C_d = THK + \delta/2 \quad \dots(2)$$

where  $\delta$  is the standard EM plane-wave skin-depth (in m) depending on the apparent conductivity (obtained by the inversion) and frequency. Essentially we have replaced the original apparent depth estimate (AD) which can take on both positive and negative values with the THK parameter returned by the inversion and which is strictly positive.

### 3 Example application to the TEL-06 survey data

The TEL-06 survey data probably represent the most challenging EM data set of the surveys conducted. They are used as an example of the procedures employed. The eastern-most area of NI contains the majority of the population and zones of infrastructure with extensive power-distribution routes. All the conurbations required high-fly conditions and the area of greater Belfast was surveyed at high elevation as a continuous and large zone. The survey also includes a large coastal zone in which transitions from low geological conductivities (e.g.  $< \sim 50$  mS/m) to seawater conductivities in excess of 1000 mS/m are observed. It should be appreciated that the modelling analysis conducted here implicitly assumes a 1D conductivity structure.

The TEL-06 EM survey data contain 2,355,137 data points (P,Q,ALT) at 4 frequencies. Here we consider only the LF (3 kHz) and HF (12 kHz) data. The inversion of the LF data produced an L1 misfit at the  $>25\%$  and  $>100\%$  error level as shown by the distributions in Figure 4a,b respectively. Some 517,296 data points (22% of total) have an error of  $>25\%$ . Some 90,072 data points (4% of total) have an error  $> 100\%$ . In the case of the higher frequency data (12 kHz), the equivalent results shown in Figure 4a,b provide 595,475 data points (25% of total) with an error of  $>25\%$  and some 147,672 data points (6% of total) have an error  $> 100\%$ .

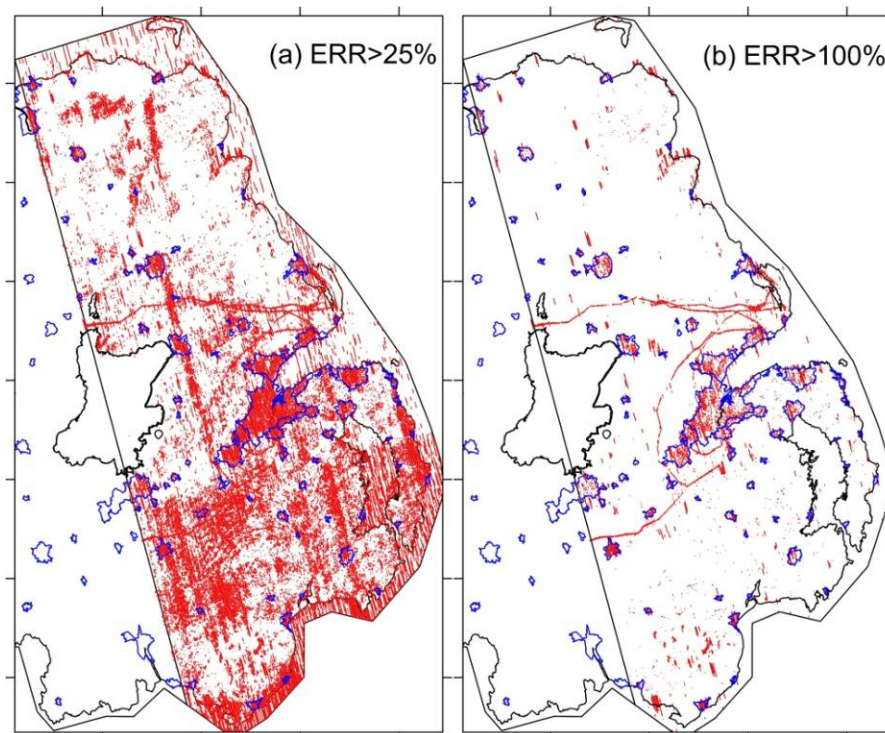


**Figure 4.** L1 misfit errors for the TEL-06 LF data. Blue areas denote urban zones. (a) Errors  $>25\%$ . (b) Errors  $> 100\%$ .

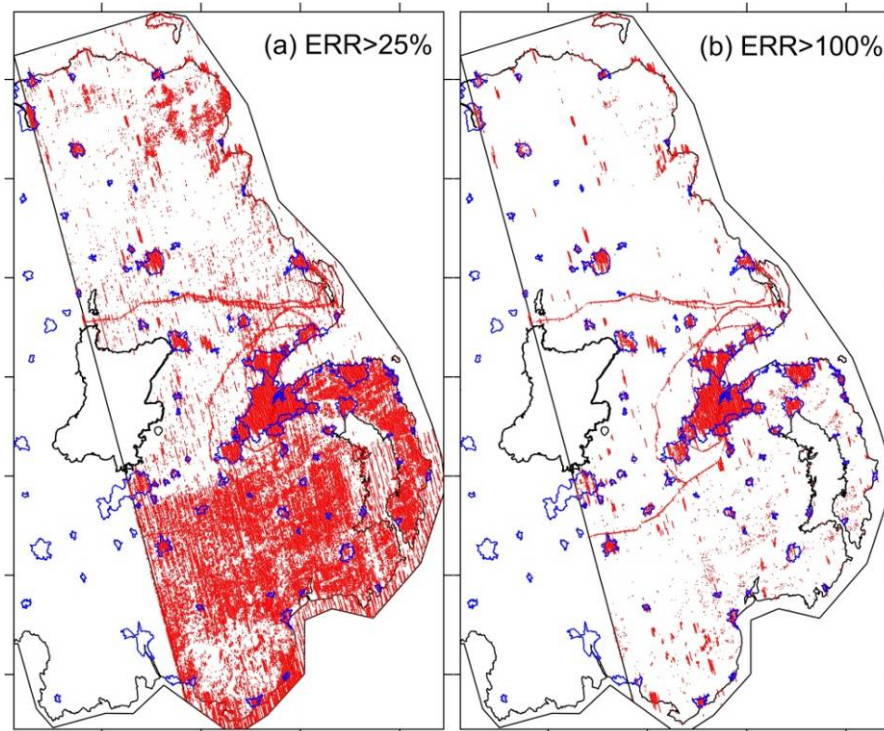


**Figure 5.** L1 misfit errors for the TEL-06 HF data. Blue areas denote urban zones. (a) Errors >25%. (b) Errors > 100%.

From Figures 4 and 5 it is evident that the higher misfits would provide a basis for culling (rejecting) invalid conductivity estimates, thus increasing the validity of the information provided. The survey zone across Lough Neagh is noticeably free of enhanced errors due to the lack of EM noise sources and relatively uniform low altitude flying. The misfits show an obvious association with towns/conurbations and areas of high-fly. The misfits > 100% identify the major cross-country power distribution grid that link to the Larne power station on the east coast. In addition there are isolated zones and individual points across the survey area that provide invalid estimates.

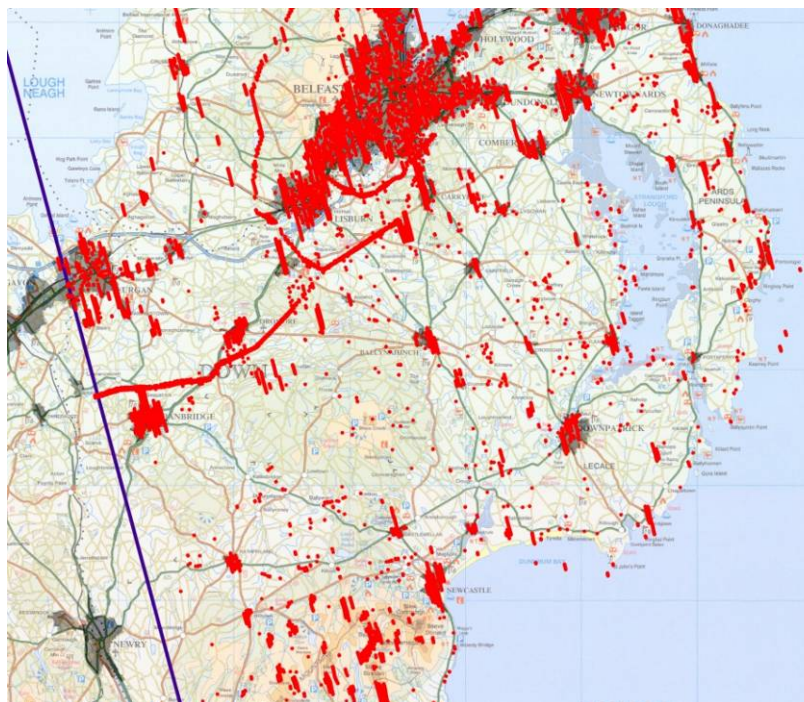


**Figure 6.** Detailed view of the L1 misfit errors > 100% for the TEL-06 LF data.

A more detailed view of the spatial distribution of misfits > 100%, at 3 kHz is shown in Figure 6. The association between conurbations and the presumed reduction in signal/noise due to high-fly (discussed below) produces zonations in the behaviour of the misfits (e.g. the Belfast conurbation). Setting these areas aside, there remain points and 'line-bursts' of enhanced misfit that can be identified and thus culled from the model data set. The line bursts include those associated with the power distribution grid. These points and bursts, when omitted, can be resampled by interpolation procedures to provide a more reliable spatial data set for geological and environmental assessment

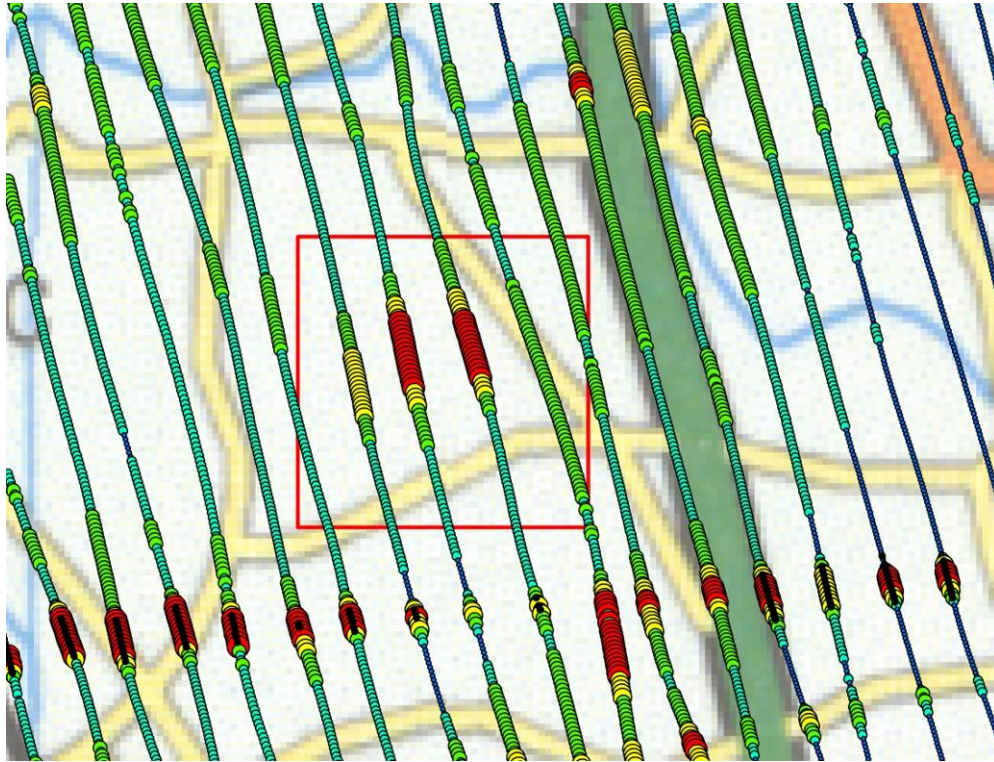


**Figure 7.** Detailed view centered on 1x1 km square (in red) of the area of the Ballymacvea landfill. Existing LF apparent conductivity shown in a 5-band colour and proportional size scheme. The highest conductivities (> 80 mS/m) are shown in red. Black symbols denote the L1 misfit > 100% zones and partially track a power-line route.

Figure 7 shows a 1x1 km square representing the location of the Ballymacvea landfill discussed by Beamish and Young (2009). To the south of this area, an E-W cross-country powerline produces misfits shown by the along-line black symbols. The coloured symbols denote the existing 3 kHz apparent conductivity shown in a 5-band colour and proportional size scheme. The highest conductivities (> 80 mS/m) are shown in red. The misfits > 100% across the area only occur in association with the powerline but it can be noted that not all powerline locations produce high misfits. The procedure of data culling will therefore not be 100% effective since it will depend on the misfit level chosen. The choice of error threshold is a necessary compromise when developing an appropriate signal/noise culling procedure for these data.

The radar altimeter data (RALT) for the total TEL-06 data set ranges from 22 to 299 m with a mean of 68 m and a median of 59 m. The behaviour of the misfit error (restricted to < 500%) and RALT at 3 kHz is shown in Figure 8. The behaviour observed at 12 kHz is very similar. The behaviour is complex but it is evident that the majority of low misfits (e.g. < 10%) are associated with the nominal height flying (~56 m). It is also apparent that misfits < 100% are largely associated with the condition RALT < 100 m. The behaviour of the misfit errors along the line of RALT=120 m is connected with a reduction in the number of iterations applied to stabilise the inversion for high-fly data.

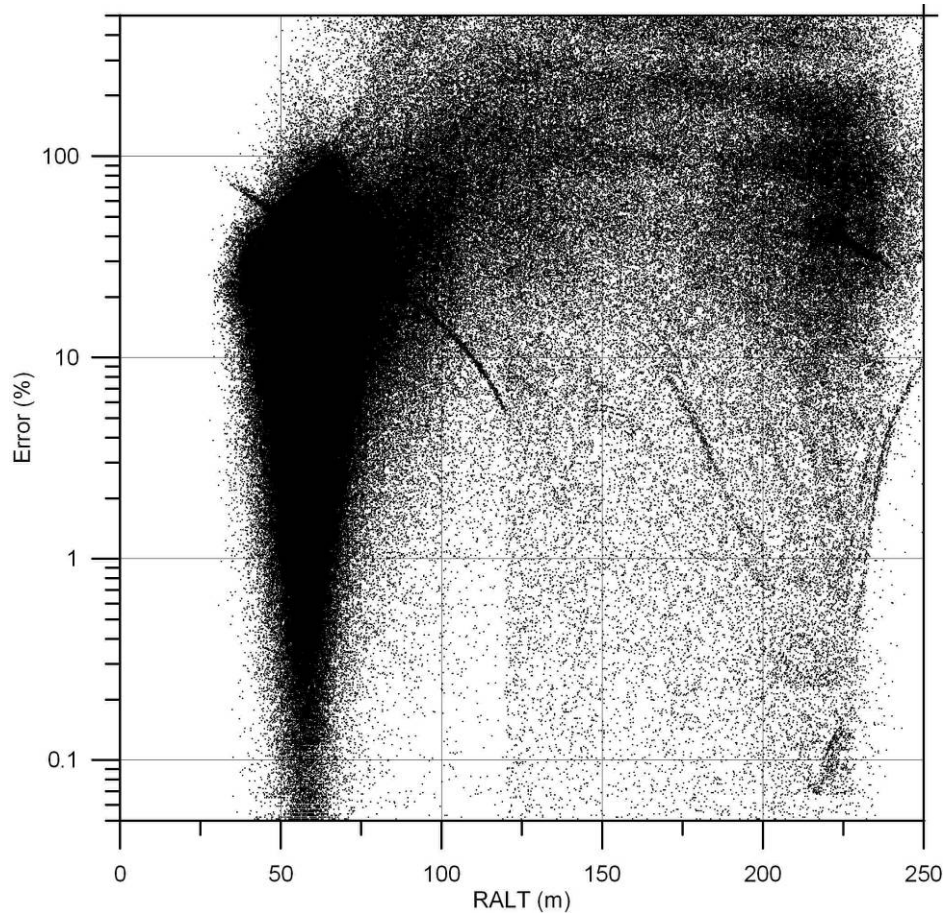


**Figure 8.** Variation of L1 misfit error (clipped to 500%) and radar altitude (RALT) for the TEL-06 LF data set.

Figure 9 shows the behaviour of the misfit error (restricted to  $< 500\%$ ) and RALT at 12 kHz using a linear error scaling. The rectangle in red defines an upper misfit limit of 100% and shows the points in the misfit cloud that would be excluded using this threshold value. In order to accommodate a further exclusion of high-fly misfit errors, the rectangle also indicates an upper threshold of 180 m (about 3 x nominal) that would further exclude a set of misfits with values  $< 100\%$ . This restriction is applied to accommodate the inconsistent behaviour of the apparent conductivity values returned across high-fly zones. The actual threshold is arbitrary but has been arrived at following studies on the delivered data sets.

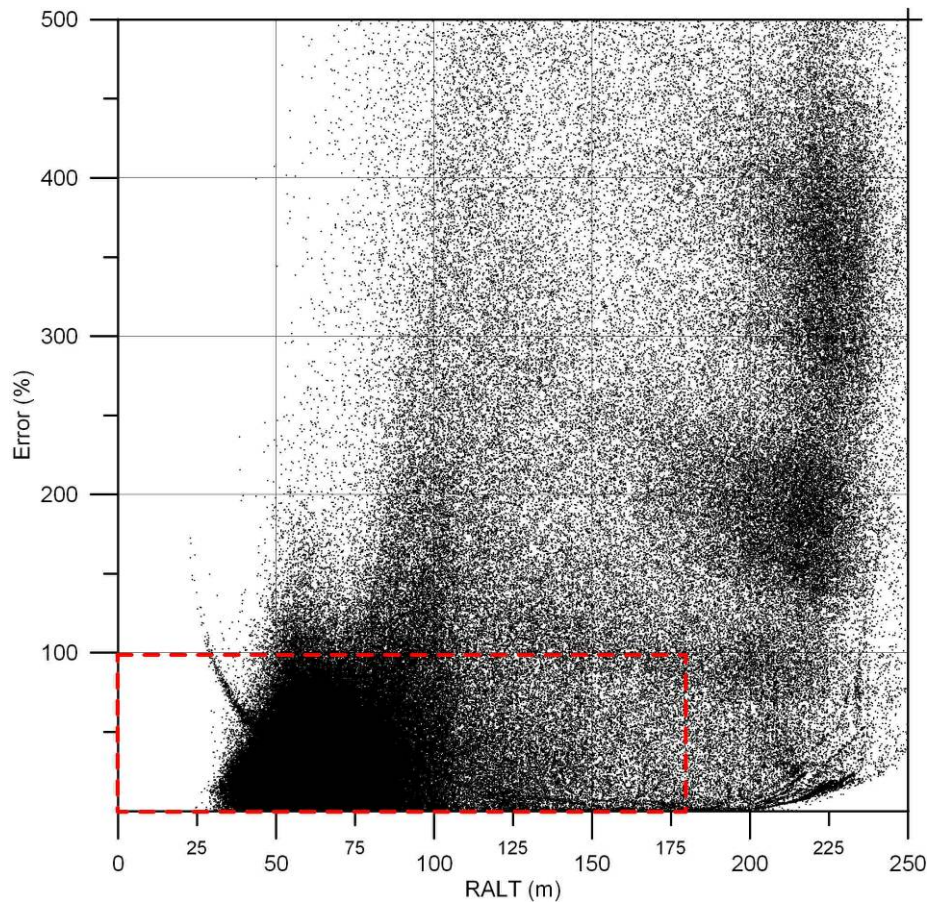


**Figure 9.** Variation of L1 misfit error (clipped to 500%) and radar altitude (RALT) for the TEL-06 HF data set.

The transform and inversion procedures are applied to (P,Q,ALT) data. The application of minimum threshold values to P,Q data sets in the case of transform procedures are described in Appendix 1. In the reprocessing/inversion of the data considered here a minimum value threshold of P,Q = 20 ppm (LF data) and P,Q = 30 ppm (HF data) has been applied. Thus if either of the P or Q values are less than the threshold value then both P and Q are set to the threshold value. This low value thresholding procedure provides limiting values in the estimates of apparent resistivity/conductivity in both transform and inversion modelling.

The transform and inversion procedures provide identical/similar estimates of apparent resistivity/conductivity when using good quality data. When complex data sets containing various noise sources are considered, significant variations become apparent. Figure 10 compares the contractor delivered apparent resistivities with those from the inversion procedure at 3 kHz for the TEL-06 data. The contractor delivered transform apparent resistivities range from 0.01 to 2749 ohm.m (see Appendix 1) and the inversion apparent resistivities range from 0.1 to 10000 ohm.m. In the latter case, lower and upper values are threshold (clip) limits applied to the results of the inversion. In Figure 10 a strong linear behaviour is observed between the two sets of estimates with a tendency for the transform value to be less than that of the inversion value. This is most apparent towards higher values of apparent resistivity. Limiting values are observed in relation to the behaviour of low amplitude (P,Q) threshold used in the 2 procedures.

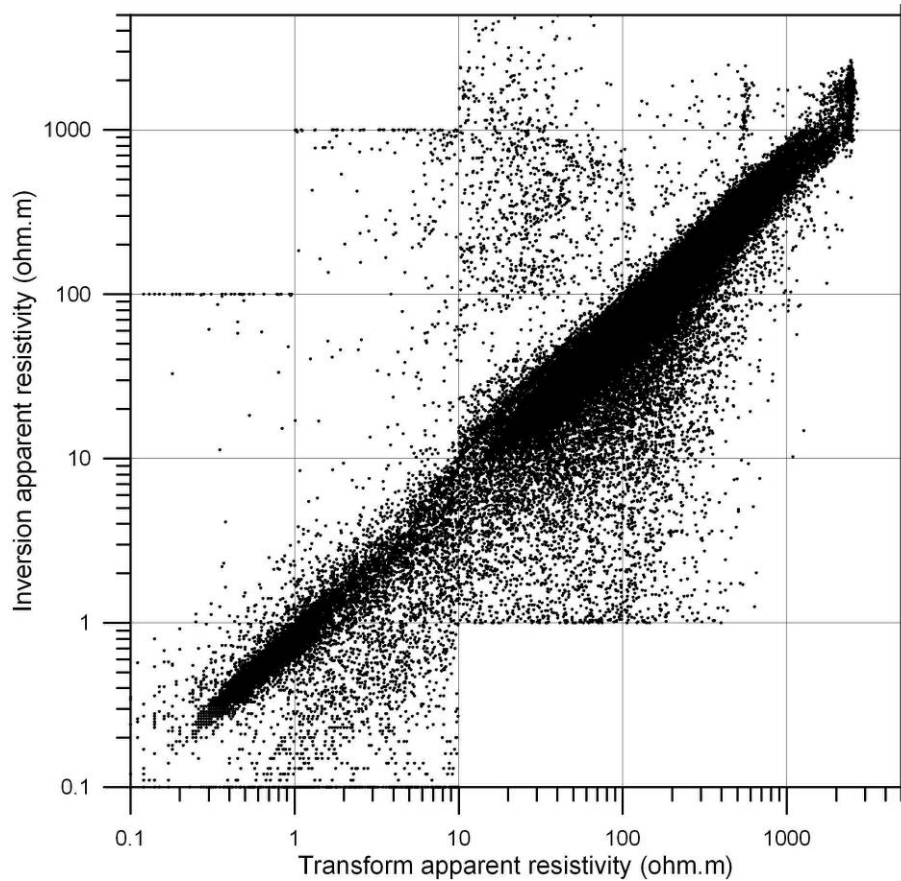


**Figure 10.** Plot of transform and inversion apparent resistivity estimates for the TEL—06 LF data.

Inverted model apparent conductivities obtained for the TEL-06 LF data using the ERR(100%) and RALT(180 m) culled data set are shown for the area around Belfast in Figure 11. Both images use an equal-area colour scale and a maximum conductivity threshold of 1000 mS/m. The image on the left is minimum-curvature (MC) grid with a cell size of 50 m. The image on the right is a natural-neighbour (NN), or ‘tinned’ grid with a cell size of 50 m. The MC grid provides min/max data values of -192/ 1177 mS/m. The NN grid provides values of 0.4/1000 mS/m and is faithful to the observed data values. The MC gridding procedure was originally intended for potential fields. Undershoot and overshoot occur in the MC grid across all sharp boundaries in the conductivity distribution. Undershoot and overshoot bleeds are most evident across power lines and at the coast but they exist at smaller scales and such edges form targets for both geological and environmental interpretation. It is concluded that the NN gridding technique is the most suitable method for gridding the EM and conductivity/resistivity data sets.

It should be noted that corrugations exist in the model and cannot be removed by either of the gridding techniques. The MC grid, as implemented in the Geosoft procedure, allows for a blanking distance and the left image contains ‘no data’ blanks across the culled portions of the data. When ‘no data’ blanks exist at scales less than the grid cell size, non-null values are returned in the grid. Elsewhere large values of culled data are defined as blank.

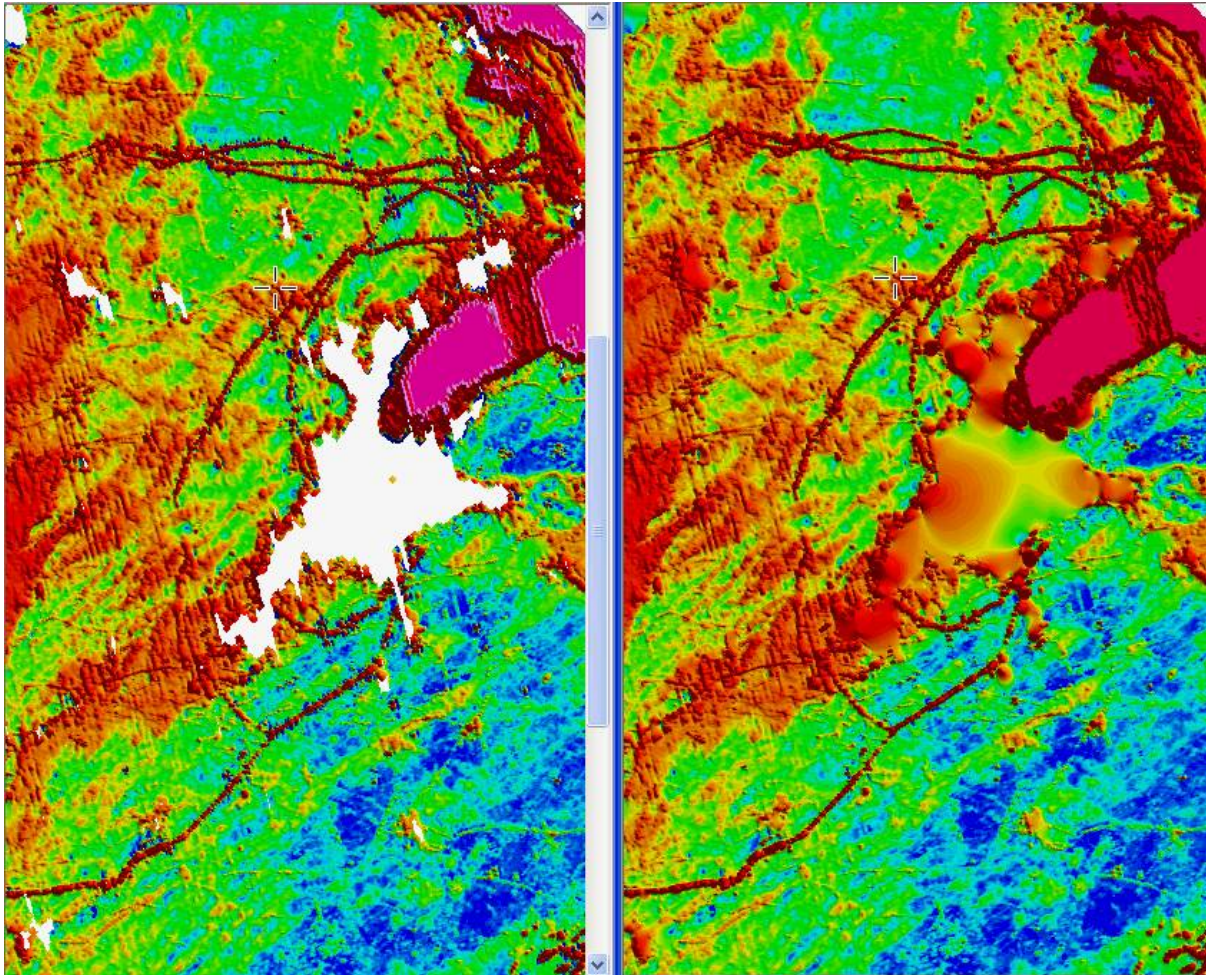


**Figure 11.** Inversion result grids (detailed area) from the TEL-06 LF data. Both images use 50 m cells and equal-area colour. (a) Minimum-curvature grid. (b) Natural-neighbour grid.

It can be noted that high conductivities are still associated with the power line routes. This is because although the central region of the perturbation is identified at an error level of 100% (e.g. Fig. 7), perturbation, ‘side-lobes’ still exist and form part of the data set that is gridded.

A natural consequence of the NN gridding procedure is that ‘no data’ blanks are filled with interpolated values. When no-data zones exist at small scales, the interpolation is advantageous. With increasing size and complexity of no data areas, the interpolation may become exotic and inappropriate.

### 3.1 DATA LEVELLING

The inversion of the P,Q,ALT data to provide best-fitting estimates of apparent resistivity generates a half-space model that may require a further degree of levelling. In the context of magnetic data this is referred to as microlevelling but with spatially focussed resistivity estimates the method of choice is the floating median difference (FMD) method described by Hautaniemi et al. (2005) and further by Mairing and Kihle (2006). The method is based on a sliding window technique and is a statistical adjustment of the data both along each flight line and across sets of adjacent flight lines. The non-linear median filter acts as a noise filter and removes any localised spikes and although it is a smoothing filter it preserves edges in the data set. In the implementation used here, the level of the correction is controlled by a linear variable so that lower values of apparent resistivity (with greater accuracy) are not corrected as heavily as high values. The procedure used is also designed to suppress the generation of negative values.

In order to apply ‘light’ levelling data adjustments, a scheme based on a window length of 1000 m along each line and a 500 m length/radius across lines (i.e. using 2 lines adjacent to each central line, a total of 5 lines) is adopted. It should be noted that the levelling is best performed on accurate data. The FMD procedure is therefore applied here to the culled data sets ( $ERR < 100\%$  and  $RALT < 180$  m) and so the rejected (poor quality) estimates of the apparent resistivity are not included in the statistical calculations. In practice the procedure works in a true distance reference frame about each point. The survey data are all flown at a nominal orientation of  $345^\circ$  so that the data are rotated to N-S to apply the FMD procedure and then subsequently rotated back to  $345^\circ$ .

The FMD levelling corrections applied to TEL-06 inverted apparent resistivities (culled data) are shown in Figure 12a in the rotated (N-S) reference frame. The images are posted colour values using a 5-band data value scheme that emphasises the small adjustment central region (-10 to +10 ohm.m) together with outlier values. The culled data set at 3 kHz (Fig. 12a) has 2,210,512 data points and the 12 kHz data set (Fig. 12b) has 2,193,131 data points. The HF data can be seen to have higher levels of adjustment than the lower frequency data. In both cases the large majority of data is adjusted only slightly. In Figure 12b, 68.2% of the data occupy the interval from -10 to +10 ohm.m with only 2.3% in the outer 2 tails (adjustments  $> 100$  ohm.m).

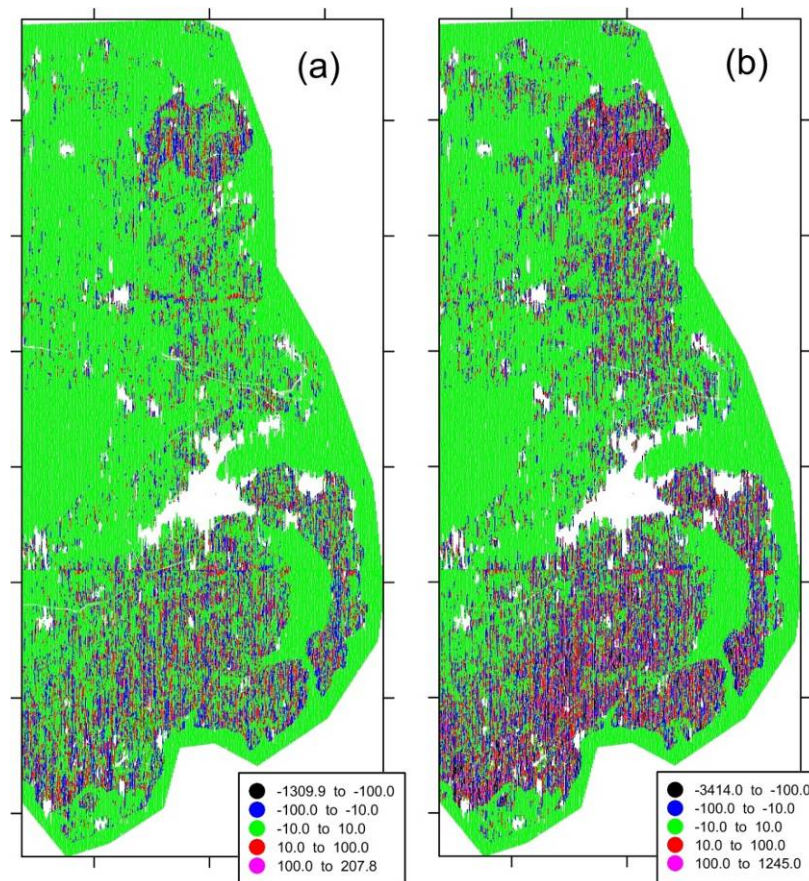


**Figure 12.** Posted value plots of the FMD levelling corrections applied to the apparent resistivity model estimates for the TEL-06 data. Rotated (N-S) reference frame. (a) LF data. (b) HF data.

The results of applying the levelling are shown, as previously, for the area around Belfast in Figure 13. It is evident that the levelling applied has resulted in an effective decorrugation of the original data set.

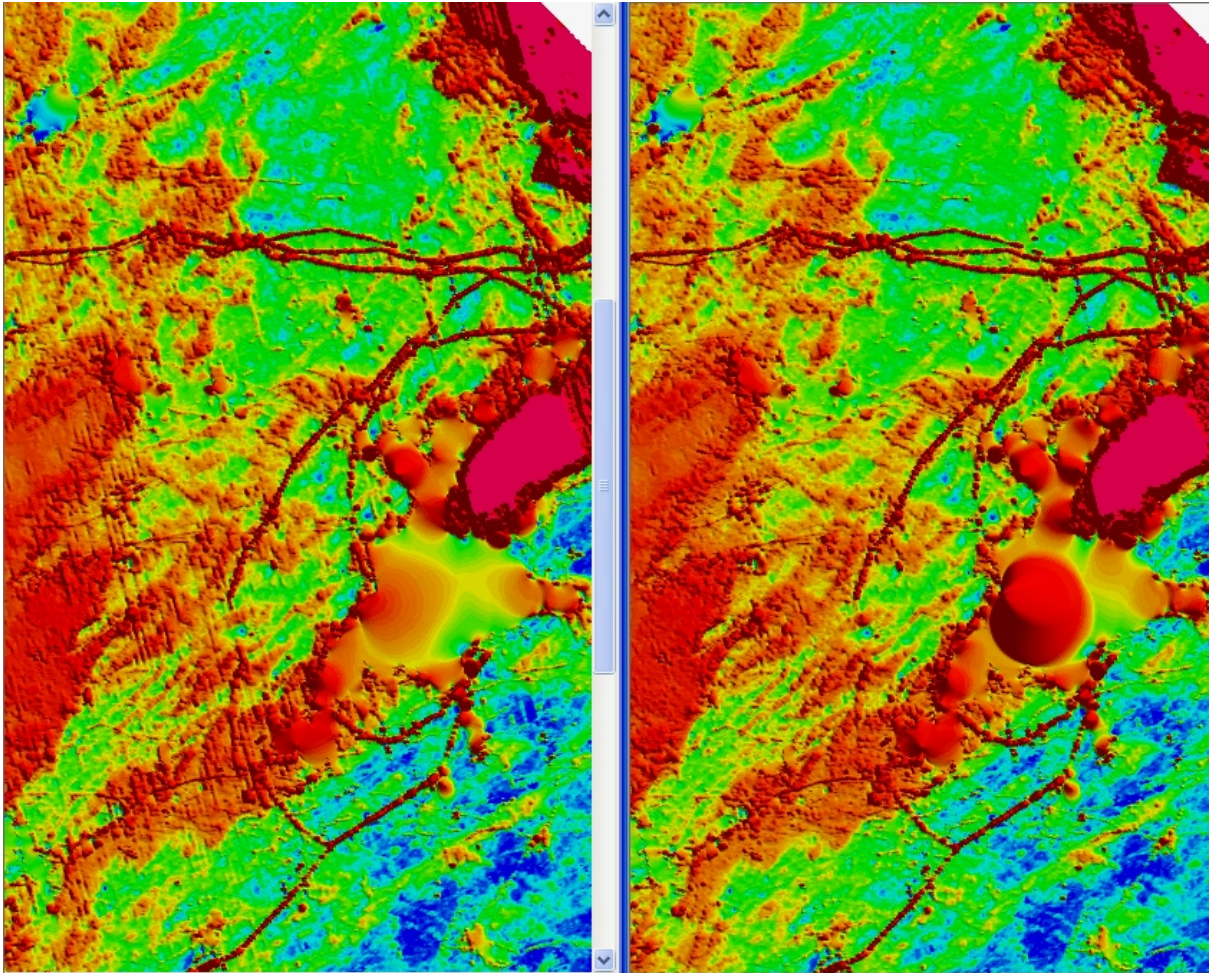


**Figure 13.** Detailed area inversion result grids (NN) from the TEL-06 LF data. Both images use 50 m cells and equal-area colour. (a) Pre-levelled data. (b) FMD levelled data.

Resolution comparisons are better demonstrated using shaded-relief images. Figure 14 shows shaded-relief images of the transform and inversion results of LF apparent conductivity in the SW of the Tellus survey in the vicinity of Enniskillen ('E' in Fig. 14a). The existing transform data clearly display a lower degree of detailed resolution than the inversion data.

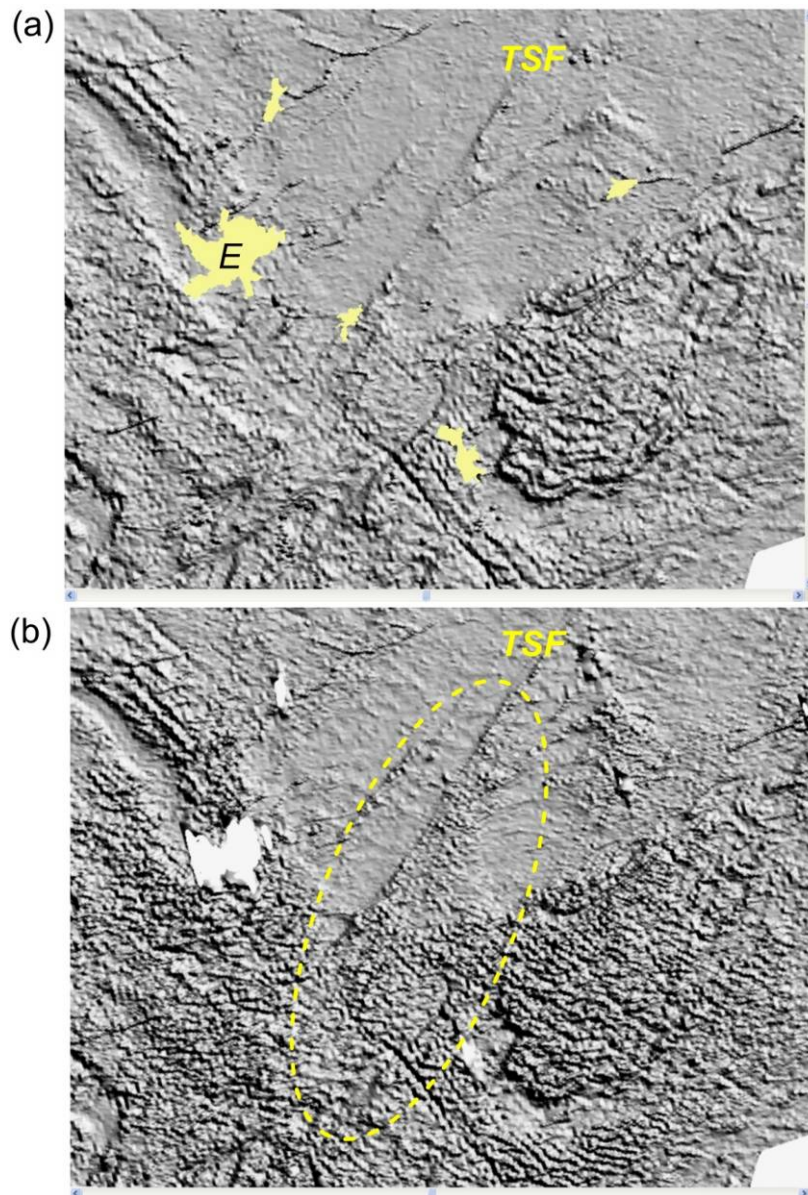


**Figure 14.** Transform (a) and inversion (b) shaded relief images of LF apparent conductivity across an area in the SW of the Tellus survey. Light source is  $+45^\circ$  from north in both cases. E refers to Enniskillen. (a) Shows towns as infilled (yellow) polygons. (b) Shows high-fly zones  $> 175$  m, as blanks. The central NE-SW structure is the Tempo-Sixmilecross Fault (TSF).

It could be argued that the lower resolution transform image is preferable since it detects only the largest of the gradients that exist, and that this ‘simplification’ is useful. The higher resolution inversion result image does however detect a possible splay structure associated with the termination of the Tempo-Sixmilecross Fault (TSF).

## 4 The Cavan Survey

The ERR results of the 2 frequency inversion applied to the CAV contractor delivered data set are shown in Figure 15a,b. The error analysis extends to a 50% threshold (i.e.  $ERR > 50\%$ ). The condition  $RALT > 180$  m is also shown in Figure 15b.

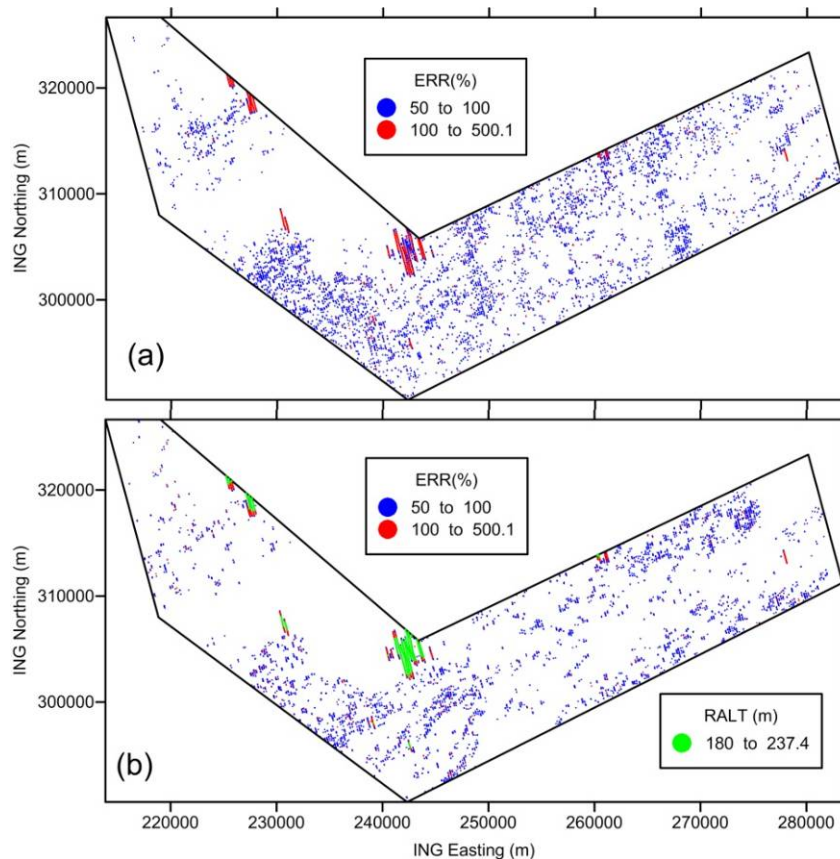


**Figure 15.** L1 misfit errors (ERR) for the CAV (a) LF and (b) HF data. Lower image (b) also shows  $RALT > 180$  m.

The major conurbation across the survey area is Cavan (north centre) and this is reflected in both ERR and RALT values. In this largely rural area there are 2506 (from a total of 338725) values with  $RALT > 180$  m. There are 14,942 values with  $ERR > 50\%$  (4% of total) in the LF data and 12,827 values (4%) with  $ERR > 50\%$  in the HF data. It can be noted that a 4% culling of the TEL-06 was performed using an error threshold of  $ERR > 100\%$ . Here we use  $ERR > 50\%$  to provide a similar level (i.e. about 4% of the data) of misfit cull.

The Cavan data were processed with a rejection level of  $ERR > 50\%$  and  $RALT > 180$  m (same RALT as previously). Following inversion, and culling, the Cavan data were levelled using the same FMD parameters as previously (1000 m along line and 500 m across line). The resulting grid images are shown in Figure 16. A detailed examination of the LF behaviour indicates that, despite the advanced processing applied, a number of high conductivity localised and presumably non-geological responses remain.

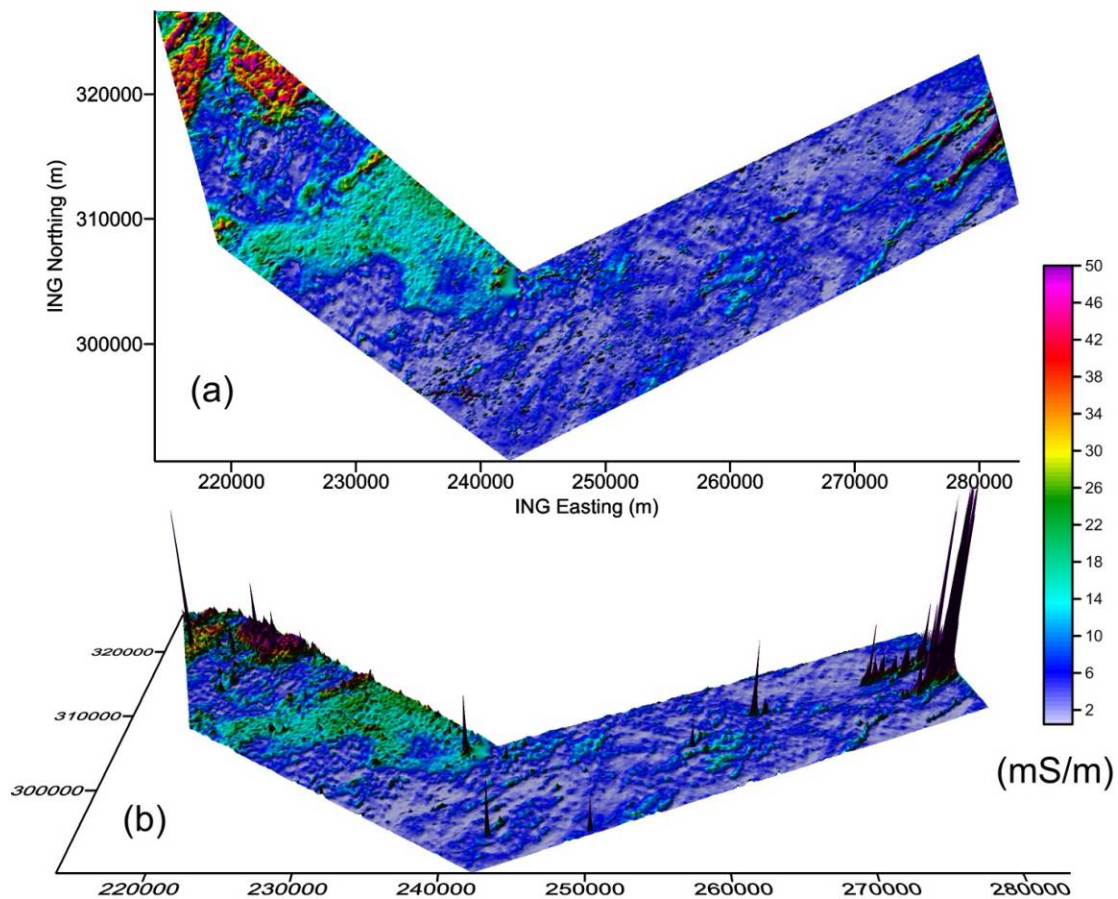


**Figure 16.** Final apparent conductivity estimates for the CAV survey at (a) LF and (b) HF. The lower image is shown as a perspective view to indicate the dynamic range of both geological (spatially sustained) and non-geological (localised) influences in the processed data set.

## 5 The Tellus Border Survey

The final contractor EM database became available for assessment on 06/12/2012. The data considered are the LF (3005 Hz) and HF (11962 Hz) apparent resistivities and their associated coupling ratios (P,Q) together with radar altitude. The smoothed final radar values (radar channel) supplied by the contractor are used here.

The area of the Conroy survey (Fig. 1) allows a comparison of the resistivity/conductivity information provided by 2 contractors and separated by ~6 years in time. The LF apparent conductivity provided by the TB survey is shown in Figure 17a. The observed conductivity variations are modest (e.g. largely < 15 mS/m) with isolated large amplitude noise spikes dispersed across the area. The JAC delivered data was gridded in precisely the same way (NN grid at 50 m) and the resulting grid was subtracted from the TB grid. The difference image is plotted in Figure 17b and is restricted to the range from +/- 4 mS/m. The difference grid actually ranges from -951 to +995 mS/m due to the noise sources. The difference grid statics indicate a median value of 0.39 mS/m which implies a very good correspondence. In detail, low/high slight amplitude modulations (in the flight line direction) are likely to be associated with differences in levelling the EM data.

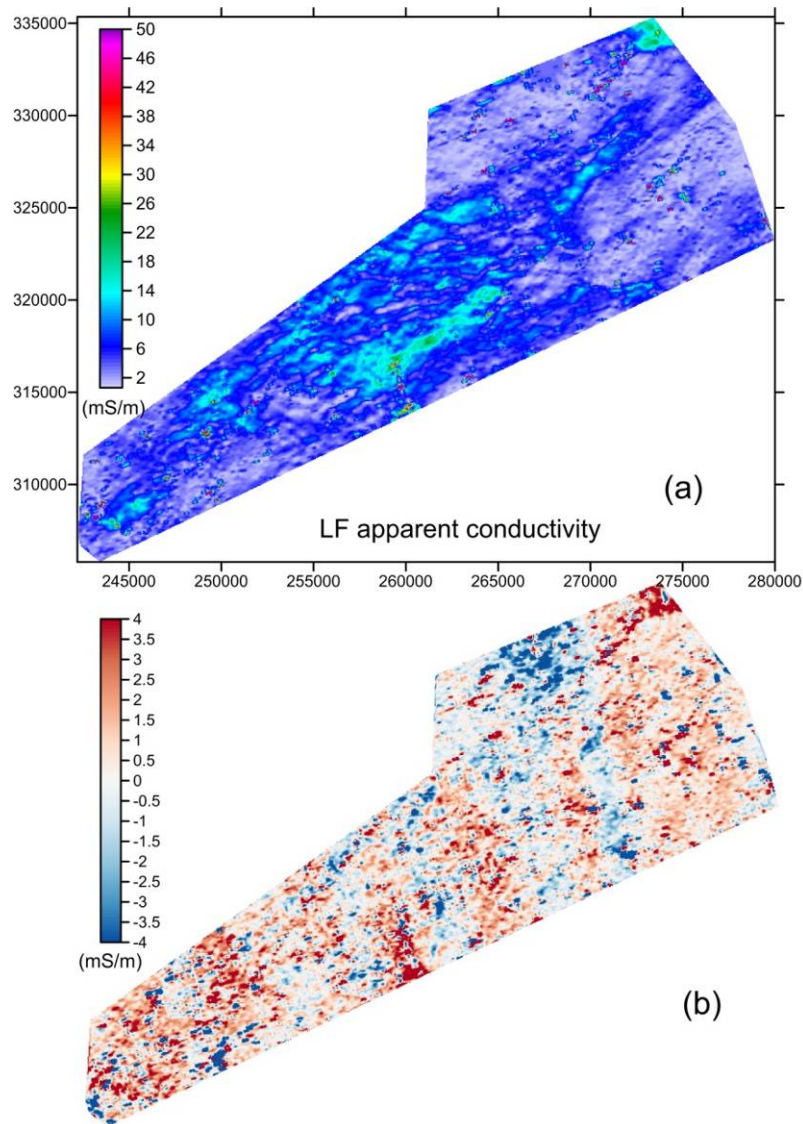


**Figure 17.** (a) TB LF apparent conductivity. (B) Difference LF apparent conductivity TB minus CONROY.

The analysis was also undertaken using the HF data sets and the equivalent results are shown in Figure 18. The TB HF conductivity variations display some higher amplitudes and less noise (in the form of spikes) than the LF data. The HF difference image (Fig. 18b) indicates a persistent zone in which TB values exceed the JAC values by  $\sim 4$  mS/m but the differences undulate in association with the conductivity variations. Despite this behaviour, median and trimmed mean values of the differences are only 1.55 and 1.83 mS/m, respectively.

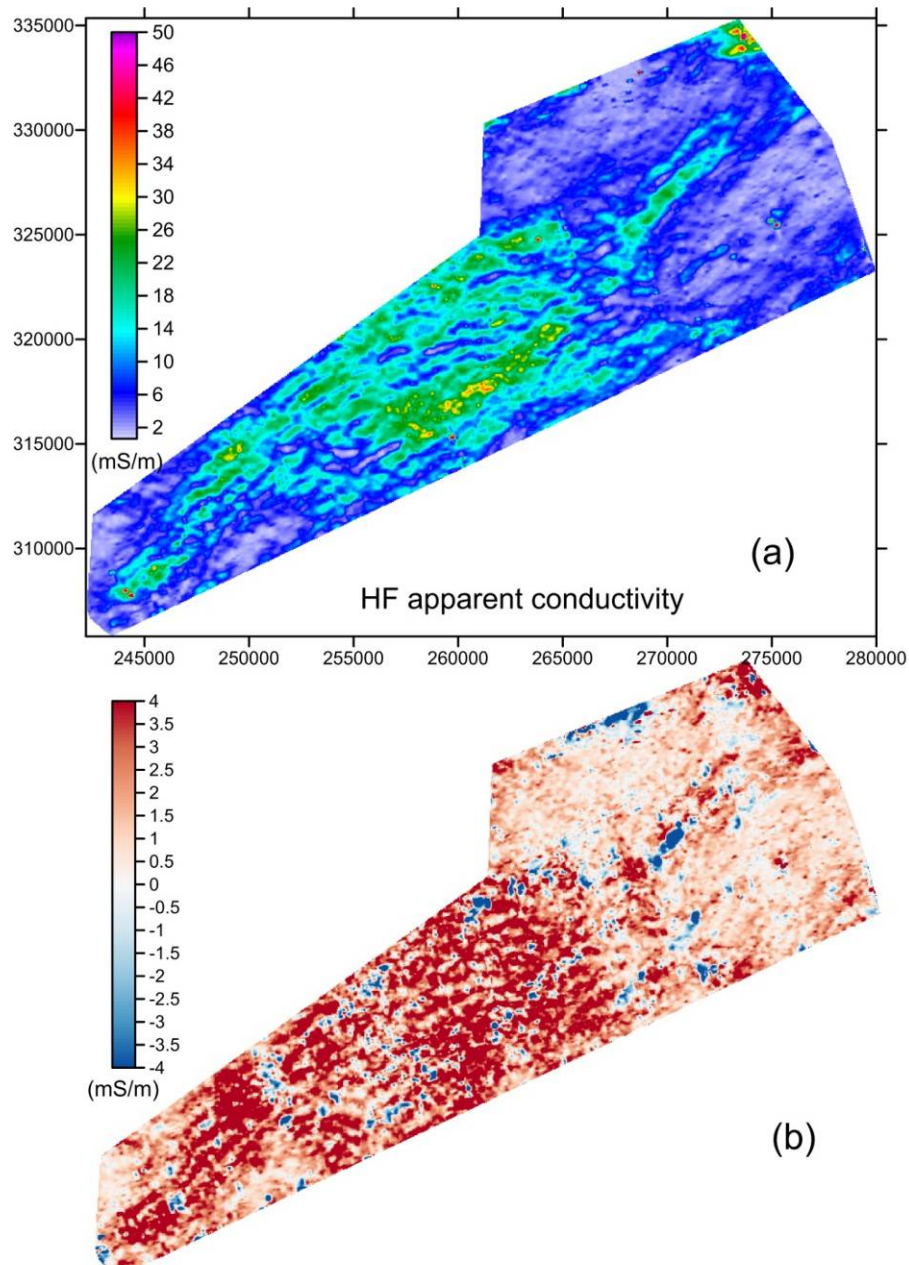


**Figure 18.** (a) TB HF apparent conductivity. (B) Difference HF apparent conductivity TB minus CONROY.

## 5.1 INVERSION OF TB DATA

The TB EM data are provided at a 10 Hz along-line sampling interval. This is a factor of 4 greater than the previous data sets sampled at 4 Hz. The typical along-line sampling was previously  $< 15$  m; the TB data are sampled at a typical distance of 6 m. Both along-line sampling intervals are much less than the lateral footprint of the EM system at the nominal survey altitude (e.g. Beamish, 2004) and it may be possible to exploit this sampling redundancy when localised errors and noise sources within the data set are more fully understood.

The contractor delivered EM data provides 9,187,435 samples across line numbers ranging from L1000 to L2021. Both the TB and OST data sets are included and are analysed jointly here. A set of lines L2001 to L2021 are from a small 100 m infill survey within the OST survey and are not included in the merging procedure considered here. The reduced data set comprises 9,177,657 data points. The radar altimeter (radar channel) ranges from a low of 26 m to a high of 791 m.

Although the TB survey was carried out across largely rural areas, the high-fly zones are a feature of the TB survey, particularly across the western area. There is therefore a zonal/swathe effect of reduced accuracy and integrity of the EM data within these areas.

As noted in the contractors report, the P,Q values were levelled with a type of FMD procedure involving a low-order polynomial model fitting of the data (Beiki et al., 2010). It is not clear how the algorithm performs in the presence of spatially-persistent high-fly errors. The delivered P,Q values were also microlevelled although the preceding FMD procedure should have removed any residual line-to-line corrugations.

As previously the inversion of the TB data provides an analysis of the variation of misfit with altitude. The behaviour of the misfit error (restricted to  $< 500\%$ ) and RALT for the LF and HF data is shown in Figure 19. The data considered is a subset of the whole data set comprising 2,605,893 data points from the initial (western) set of lines L1000 to L1300.

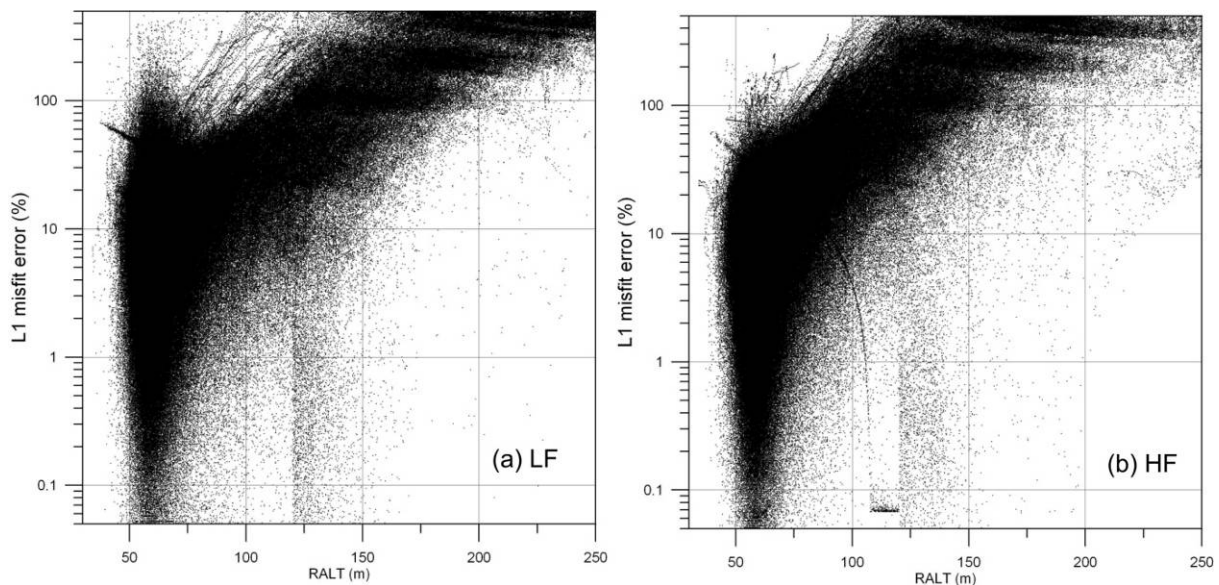


**Figure 19.** Variation of L1 misfit error (clipped to 500%) and radar altitude (RALT) for the TB data set Lines L1000 to L13000. (a) LF and (b) HF.

For practical purposes (efficiency of grid construction) the TB data set was split into 2 (west and east) subsets for processing. The western subset comprised Lines 1000 to 1480 and the eastern subset comprised Lines 1481 to 1946. Five lines of overlap (for merging) between the 2 subsets were also introduced.

For the combined TB dataset (Lines 1000 to 1946, no overlap) the inversion result statistics providing the standard culling rejection limits of  $ERR > 100\%$ ,  $RALT > 180.0$  m together with the combined rejection statistics are given in Table 2.

**Table 2.** Statistics (number of values and percentages of total) of the TB inversion results using standard rejection criteria of  $ERR > 100\%$  and  $RALT > 180$  m, together with their combined rejection statistics.

	N	ERR>100%	RALT>180 m	Combined
LF	9,176,994	832,522 (9%)	633,715 (7%)	879,691 (9.6%)
HF	9,176,994	1,037,391 (11%)	633,715 (7%)	1,070,647 (11.7%)

It is suggested that the higher levels of rejection observed in the TB data are due to the higher sampling interval ( $\times 4$ ) of these data. An example of the misfit and RALT behaviour across the

western subset is shown in Figure 20. An example of the misfit and RALT behaviour across the eastern subset is shown in Figure 21.

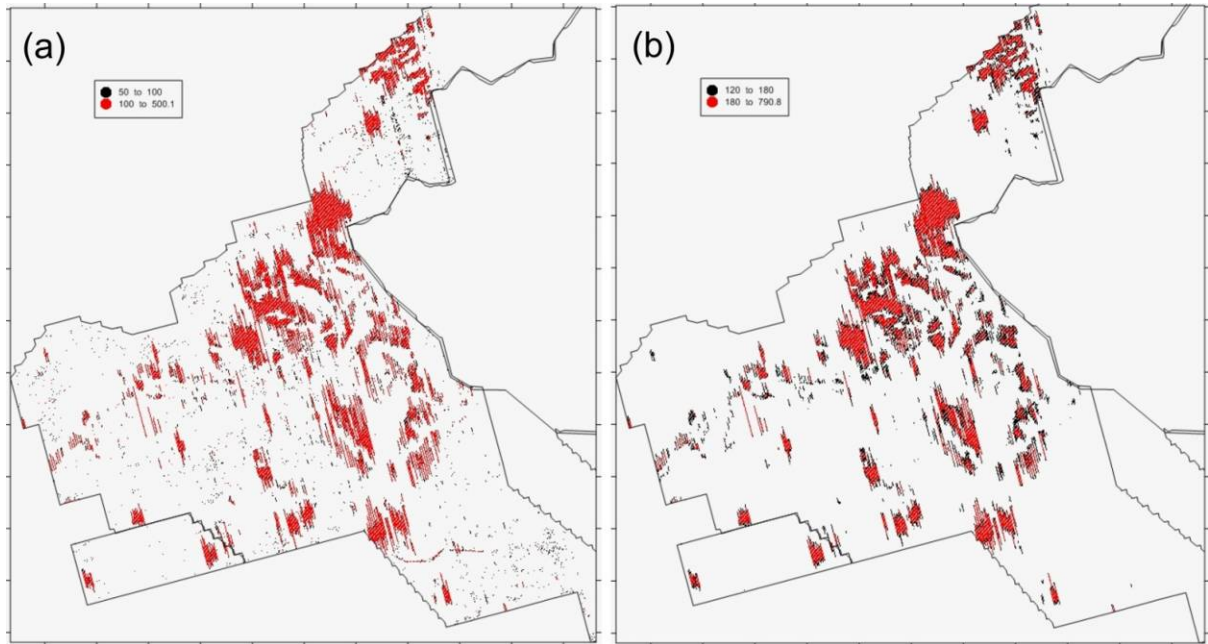


**Figure 20.** (a) Observed L1 misfit errors for the TB LF western data (5-100% in black, 100 to 500% in red). (b) RALT for the TB western data (120 to 180m in black, 180 to 791m in red).

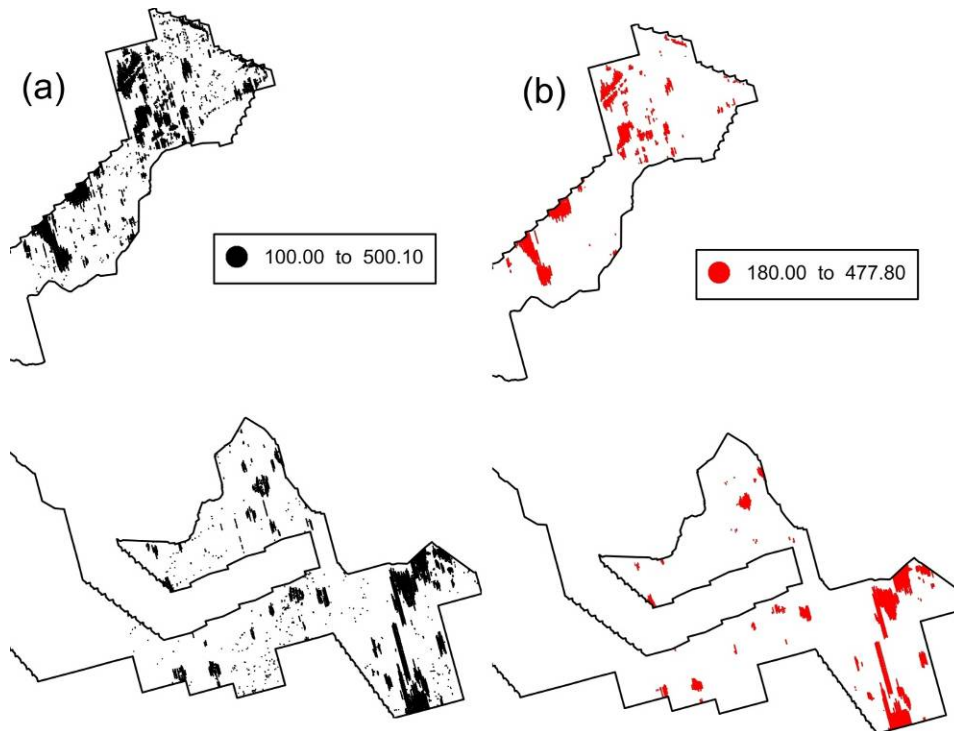


**Figure 21.** (a) Observed L1 misfit errors for the TB HF eastern data (values>100%). (b) RALT for the TB eastern data (Values>180m).

## 6 Merging the 4 data sets (grids)

The general merging procedure adopted was to move the data sets ‘forward in time’ so that the latest data set (TB) remained static and previous survey data (TEL-05, TEL-06 and Cavan) were sequentially adjusted, as appropriate. The contractor delivered coupling ratios (P,Q) and radar altitude (RALT) formed the basis of the procedure. The full procedure involved:

- Inversion of the (P,Q,RALT) data as described previously, for each of the surveys. This procedure provided estimates (a model) of half-space conductivity, the L1 inversion misfit error and the thickness of an at-surface resistive zone, overlying the half-space.
- Examination of the L1 misfit errors (ERR) and high-fly zones. A standard combined rejection criteria of  $ERR > 100\%$  and  $RALT > 180$  m was adopted to cull poor-quality estimates of the half-space conductivity. The procedure produced a revised, reduced data set containing data gaps from single points, clusters of points and zones, as described previously.
- The apparent resistivity estimates from the reduced data set were subjected to a FMD method of levelling involving a window length of 1000 m (along line) and a 500 m length/radius across lines (i.e. using 2 lines adjacent to each central line, a total of 5 lines). The procedure was applied in a N-S rotated coordinate system. The procedure adopted ensured that the poor-quality model estimates did not contribute to the levelling of the data.
- The levelled data (with gaps) were used to create a 50 m grid using a natural neighbour (NN) algorithm. This gridding procedure accounts for edge effects in the data and returns values precisely within the bounds of the observed data (no negatives and excessive positive values due to under and over shoots). Prior to NN gridding, apparent conductivity values were clipped to a maximum value of 1000 mS/m. This thresholding procedure restricts both offshore conductivities and isolated outliers (spikes) and allows for more accurate gridding/imaging. The NN grids are unrestricted at low values of apparent conductivity
- The NN procedure provides an interpolation across all the gaps within the data set. The interpolation is effective when the gaps are small and close natural neighbours exist. When the gaps are extensive and no close natural neighbours exist, the interpolation becomes exotic (unrealistic). The levelled NN grids form the basis for the merging procedure.

### 6.1 MERGING TEL-05 AND TEL-06

As noted previously, different frequencies were employed at LF and HF during the Tellus surveys. In order to estimate an appropriate offset, 2 repeated survey lines (L1214 and L1215) were employed. The inverted model data from the two repeat lines were used to assess the DC level adjustments required to adjust the TEL-05 model parameters to fit those of the TEL-06 parameters. The adjustments were found to be as follows:

- Apparent conductivity: LF. A value of 2.47 mS/m was added to the TEL-05 LF data.
- Apparent conductivity: HF. Although the analysis indicated a subtraction of 2.50 mS/m to the TEL-05 results, this was found to produce extensive areas of negative values. No adjustment to the TEL-05 HF data was performed.
- There is no adjustment applied to the ERR or THK model parameter.

Merging of the TEL-05 and TEL-06 grid results was undertaken using the Geosoft extension GridKnit module. An automatic suture method was applied using a no static and no trend adjustment condition. The resulting merged grids (LF and HF) are referred to as TEL-05-06.

Comparisons were undertaken between existing transform and inversion estimates of the LF and HF apparent conductivities. The existing ‘whole Tellus’ estimates were obtained from the contractor supplied Version 2 data file (emap\_v2.xyz, 2006). Figure 22 shows a comparison across the northern coastal area centred on Magilligan Point and part of the TEL-05 data set. The images shown are LF apparent conductivity (NN grids at 50 m) obtained by the transform (Fig. 22a) and by the inversion method (Fig. 22b) considered here. Both data sets are clipped to the coast and use the same linear colour scale restricted to a high value of 100 mS/m.

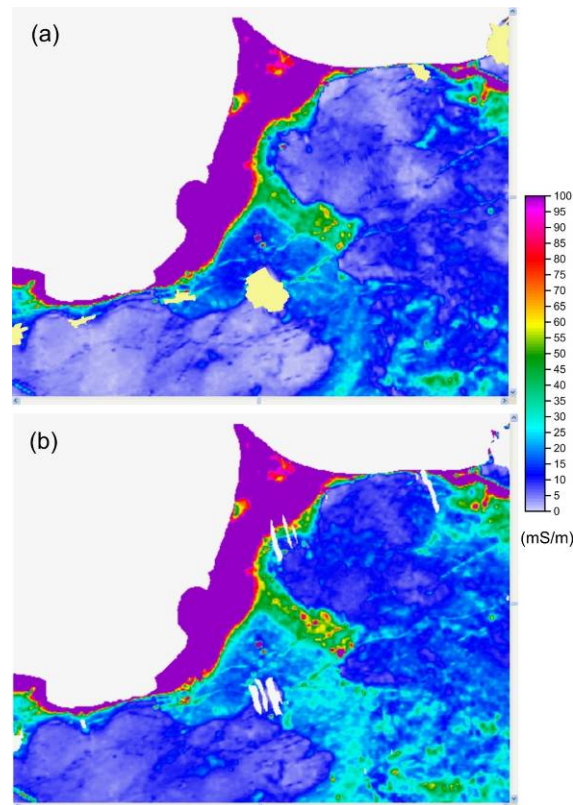


**Figure 22.** Transform (a) and inversion (b) images of TEL-05 LF apparent conductivity across an area centred on Milligan Point. (a) Shows towns as infilled (yellow) polygons. (b) Shows high-fly zones > 175 m, as blanks (white areas). Images are cut to coast.

It can be seen that that the two sets of results are broadly similar with the same hard-edges (rapid changes in gradient) identified. More subtle differences are however evident relating to the amplitudes of the variations. Two methods of identifying high-fly zones are demonstrated. Figure 22a uses an overlay polygon mask of towns, while Figure 21b identifies (with blanks) only those zones with  $RALT > 175\text{m}$ . The latter is obviously a more accurate description of the actual flying behaviour.

## 6.2 MERGING CAV AND TB

No overlap exists between the merged TEL-05-06 data sets and the CAV data. The CAV data were therefore merged with the TB data set which was designed to provide an adequate overlap with the CAV survey area. The CAV area is effectively a hole within the larger TB area. Merging of the CAV and TB grid results was undertaken using the Geosoft extension GridKnit module. An automatic suture method was applied using a static correction to the CAV grid only and a no trend adjustment condition. The merging result was found to be adequate and the resulting grids (LF and HF) are referred to as CAVTB.

### 6.3 MERGING TEL-05-06 AND CAVTB

The TB survey was designed to provide an adequate overlap with the existing TEL-05-06 survey area. In principle, the merged TEL-05-06 data has been adjusted to fit the actual frequencies (3005 Hz and 11962 Hz) used in the TB survey. Merging of the TEL-05-06 and TB grid results was undertaken using the Geosoft extension GridKnit module. An automatic suture method was applied using no static corrections and no trend adjustment, since this method proved the most effective.

The final merged result is a NN 50 m grid that contains a small number of negative values introduced during the merging procedure. The final merged grid obtained at LF is shown in Figure 23 with the suture lines from grid merging displayed in white. It can be seen that the merging is broadly satisfactory. The equivalent result obtained at HF is shown in Figure 24.

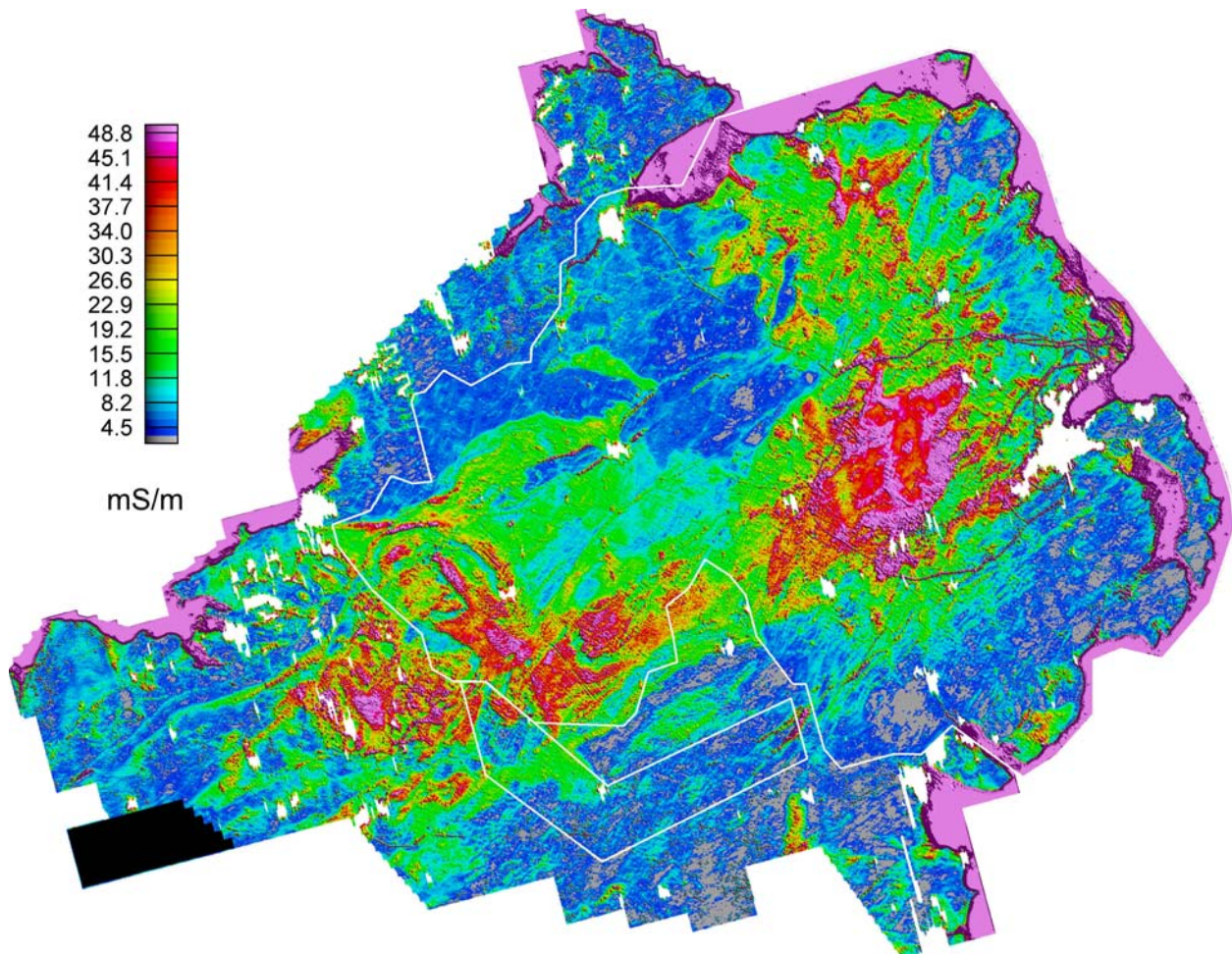


**Figure 23.** LF merged conductivity grid imaged using a linear colour scale (2 to 50 mS/m) with condition  $RALT > 175m$  defined by white zones. White lines denote survey boundaries. Black area denotes OST survey.

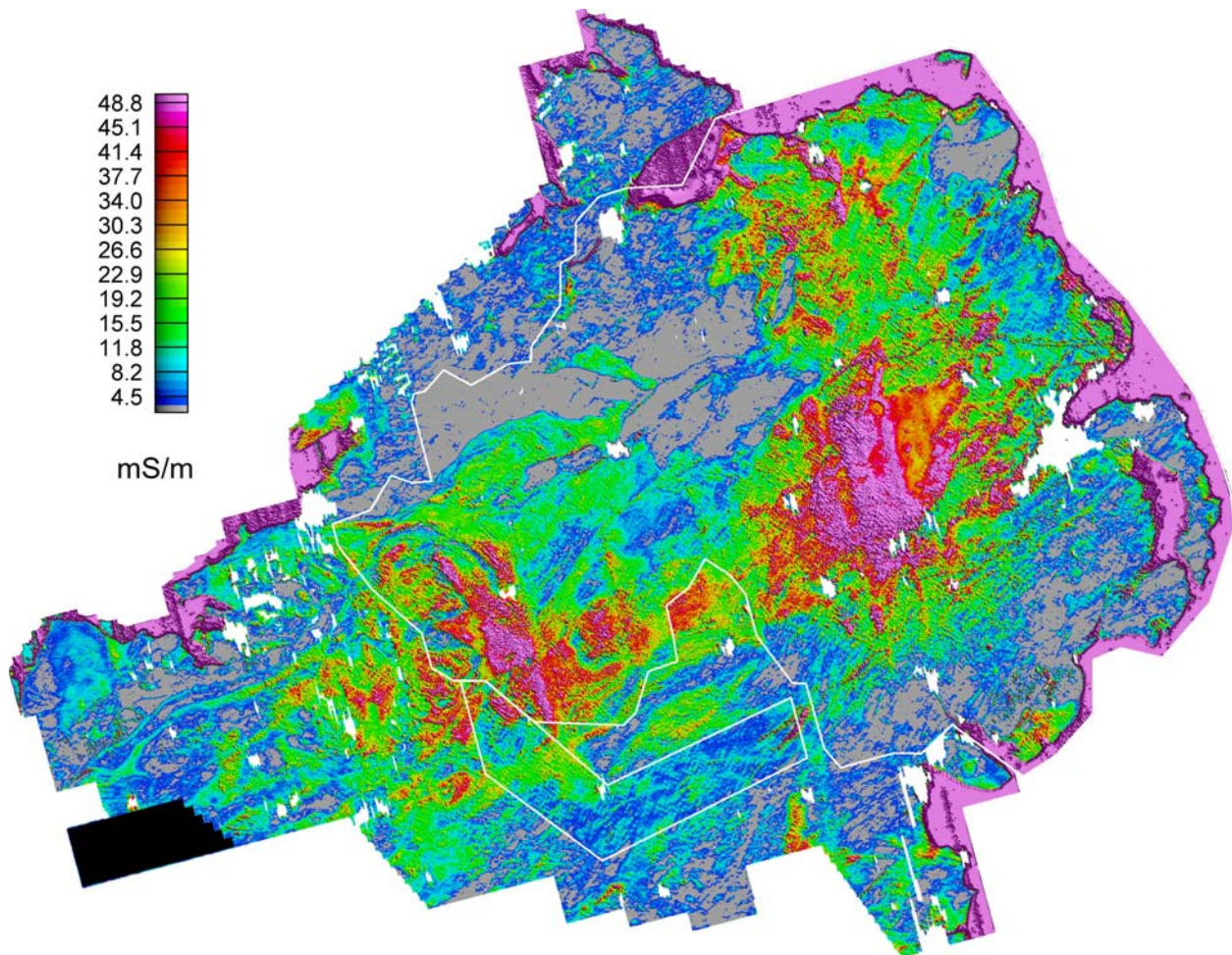


**Figure 24.** HF merged conductivity grid imaged using a linear colour scale (2 to 50 mS/m) with condition  $RALT > 175m$  defined by white zones. White lines denote survey boundaries. Black area denotes OST survey.

Most of the problems of the merging process are associated with low values of conductivity and this is because of the reduced signal/noise ratio in the resulting observed coupling ratios. The effect increases with decreasing frequency (Appendix 1). EM data obtained across resistive zones are difficult to level, and this may result in residual effects (small amplitude undulations) that can be observed in *all the data* along the flight line direction of  $345^\circ$ . These larger scale effects are associated with the resistive aperture of the EM system employed, as discussed in Appendix 1.

## 7 The merged conductivity database

The procedures discussed above resulted in LF and HF merged NN grids obtained using a 50 m cell size. This cell size is larger than the along-line distance of the original data but has resulted in a uniform sampling of all the LF and HF data. The inversion results comprising the L1 misfit error (ERR), and the thickness parameter (THK) are also available at the original sampling interval. A master EM sampling database was constructed using the original contractor supplied EM data files. The X (easting) and Y (northing) coordinates from each survey in the Irish national Grid were used. WGS84 Latitude (LAT) and Longitude (LONG) were then obtained by transformation of the X,Y coordinates.

The data base was constructed to avoid any overlaps between the surveys. Survey lines therefore ‘abut’ at the boundaries between surveys. As noted previously, the master database contains line deviations and line overlaps that were contained within the individual surveys. The master database carried forward the DATE (YYYYMMDD), the radar altimeter (RALT) and the GPS

height above geoid (WGS84) of each measurement. An additional data channel (Survey Identifier, SID) was introduced to define the survey (TEL=Tellus, CAV=Cavan and TB=Tellus Border). Line numbers from the original surveys were retained but with a prefix of B (for the Tellus Border survey), D (for the Cavan survey) and L (for the Tellus survey). The control master database constructed here provides 14,765,595 data points from 138.5k line-km of data (including the OST survey).

The master database was then populated with the LF and HF estimates of apparent conductivity from the final merged 50 m, NN grids using a grid sampling procedure. The ERR and THK inversion parameters were sampled, at their original sampling interval, into the master database. As noted previously the ERR term is restricted to a maximum value of 500%. The HF ERR is found to have a higher central moment than the LF ERR when examined across the whole data set. The thickness parameter is limited to the range  $0.1 < \text{THK} < 100.0$ . Both ERR and THK parameters are unlevelled.

The merging procedure produced a small number of spurious negative values into the values of apparent conductivity (-29.9 mS/m at LF and -200 mS/m at HF). Both data sets extend beyond the threshold maximum value of 1000 mS/m, again due to the merging procedure. When use is made of the merged apparent conductivity information it is recommended that that estimates of apparent conductivity when  $\text{RALT} > 175$  m be either omitted (see Figure 25) or treated with caution due to the procedures employed here. Finally the variable sampling interval contained in the master database (see Table 1) should be noted since it is not explicit in the information supplied.

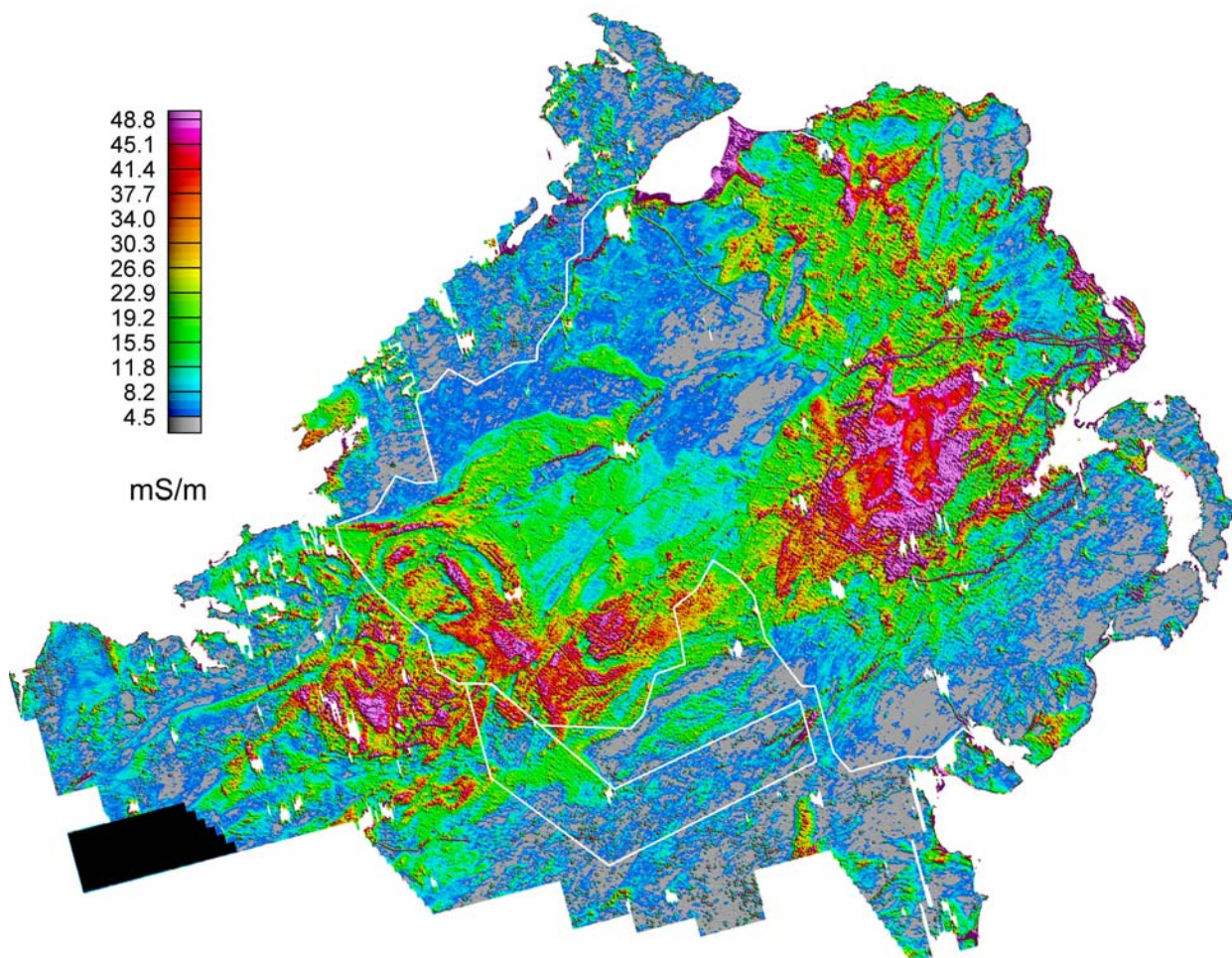


**Figure 25.** LF merged conductivity grid imaged using a linear colour scale (2 to 50 mS/m) with condition  $\text{RALT} > 175\text{m}$  defined by white zones and all data cut-to coast. Black area denotes OST survey.

## 8 References

British Geological Survey holds most of the references listed below, and copies may be obtained via the library service subject to copyright legislation (contact [libuser@bgs.ac.uk](mailto:libuser@bgs.ac.uk) for details). The library catalogue is available at: <http://geolib.bgs.ac.uk>.

- BEAMISH, D., 2002a. An assessment of inversion methods for AEM data applied to environmental studies. *Journal of Applied Geophysics*, **51**, 75-96.
- BEAMISH, D., 2002b. The canopy effect in airborne EM. *Geophysics*, **67**, 1720-1728.
- BEAMISH, D., 2004. Airborne EM skin depths. *Geophysical Prospecting*, **52**, 439-449.
- BEAMISH, D., CUSS, R.J., & LAHTI, M., 2006. The Tellus airborne geophysical survey of northern Ireland: final processing report. *British Geological Survey Technical Report IR/06/136*. A report prepared for the DETI, Belfast.
- BEAMISH, D. & LEVÄNIEMI, H., 2010. The canopy effect in AEM revisited: investigations using laser and radar altimetry. *Near Surface Geophysics*, **8**, 103-115.
- BEAMISH, D. & YOUNG, M., 2009. Geophysics of Northern Ireland: the Tellus effect. *First Break*, **27**, 43-49.
- BEARD, L.P., 2000. Comparison of methods for estimating earth resistivity from airborne electromagnetic measurements. *J. appl. Geophys.*, **45**, 239-259.
- BEIKI, M., BASTANI, M. & PEDERSEN, L.B., 2010. Leveling HEM and aeromagnetic data using differential polynomial fitting, *Geophysics*, **75**, L13-L23.
- FRASER, D. C., 1978, Resistivity mapping with an airborne multicoil electromagnetic system: *Geophysics*, **43**, 144–172.
- HAUTANIEMI, H., KURIMO, M., MULTALA, J., LEVÄNIEMI, H. & VIRONMÄKI, J., 2005. The ‘three in one’ aerogeophysical concept of GTK in 2004. Geological Survey of Finland, Special paper **39**, 21-74.

LEVÄNIEMI, H, BEAMISH, D., HAUTANIEMI, H., KURIMO, M. SUPPALA, I., VIRONMÄKI, J., CUSS, D., LAHTI, M. & TARTARAS, E., 2009. The JAC airborne EM system AEM-05. *Journal of Applied Geophysics*, **67**, 219-233.

MAURING, E. AND KIHLE, O. 2006, Leveling aerogeophysical data using a moving differential median filter: *Geophysics*, **75**, L5–L11.

SIEMON, B. 2001. Improved and new resistivity-depth profiles for helicopter electromagnetic data. *Journal of Applied Geophysics*, **46**, 65-76.

## Appendix 1.

The following notes are taken from a previously unpublished JAC document referring to the use of software (TRANSAEM07) used to convert AEM coupling ratios to estimates of apparent resistivity.

### Background

The GTK/JAC program TRANSAEM is used to calculate 2 parameters of a half-space conductivity model. The program uses the in-phase (P) and quadrature (Q) coupling ratios (in ppm), together with sensor elevation (e.g. RALT=HT) of single frequency EM data and calculates: (i) apparent resistivity and (ii) apparent depth, of the half-space.

The method follows the principles introduced by Fraser (1978). The method is a transform/look-up/nomogram (any of these terms could be used) procedure. In principle the apparent resistivity calculation could use a various combinations of observed data: (P, HT), (Q, HT) or, since we have a complex response (AMP, HT), (PHASE, HT) or (AMP, PHASE) where AMP and PHASE refer to the complex response equivalent to P and Q. The various methods are discussed by Fraser (1978) and Beard (2000).

In order to avoid introducing elevation errors into the estimation, TRANSAEM uses P and Q to estimate apparent resistivity and then P and Q are used to estimate HT. Apparent depth is calculated as the difference between observed and estimated HT.

The basis of the calculation is a look-up table which is calculated once for each frequency. The calculation uses an established forward modelling algorithm to determine the response (e.g. P and Q) of a particular coil-coil system (e.g vertical coplanar coils at a fixed separation and frequency) to a uniform half-space. The response is calculated across a fixed range of altitudes (HT parameter) and resistivities.

The files defining the look-up tables for the 4 frequency JAC system were named: ri\_two912.dat to ri\_two24510.dat. The nomograms (in P & Q) were produced by sampling in Altitude and Resistivity as shown in Figure A25. The number of points used was 2236, and a different sampling was employed for each frequency. A more dense and wider sampling is used in TransAEM07, as discussed later.

The nomograms used by TRANSAEM are shown in Figure A26, many of the points are identical across the 4 frequencies. Given a particular pair of P & Q values, TRANSAEM used these nomograms to:

- a) Estimate AP resistivity and altitude (e.g. Figure A27). The method(s) of interpolation used are not known to us.
- b) If either or both the P,Q values were outside the range of the defined nomogram, we think that the value(s) were revised to a value on the 'edge' of the nomogram.

### TRANSAEM07

As indicated in Figure A27, revised nomograms were constructed using a linear altitude range from 16 to 240 m (in intervals of 2 m). In order to 'expand' the range of low P&Q value sampling in the nomogram, a further 11 heights were added between 250 and 350 m (10 m intervals). The resistivity sampling was from 0.001 ohm.m to 80,000 ohm.m using a uniform logarithmic sampling interval of 20 points per decade. The resulting nomogram has 19716 points and the same sampling is used for all 4 frequencies.

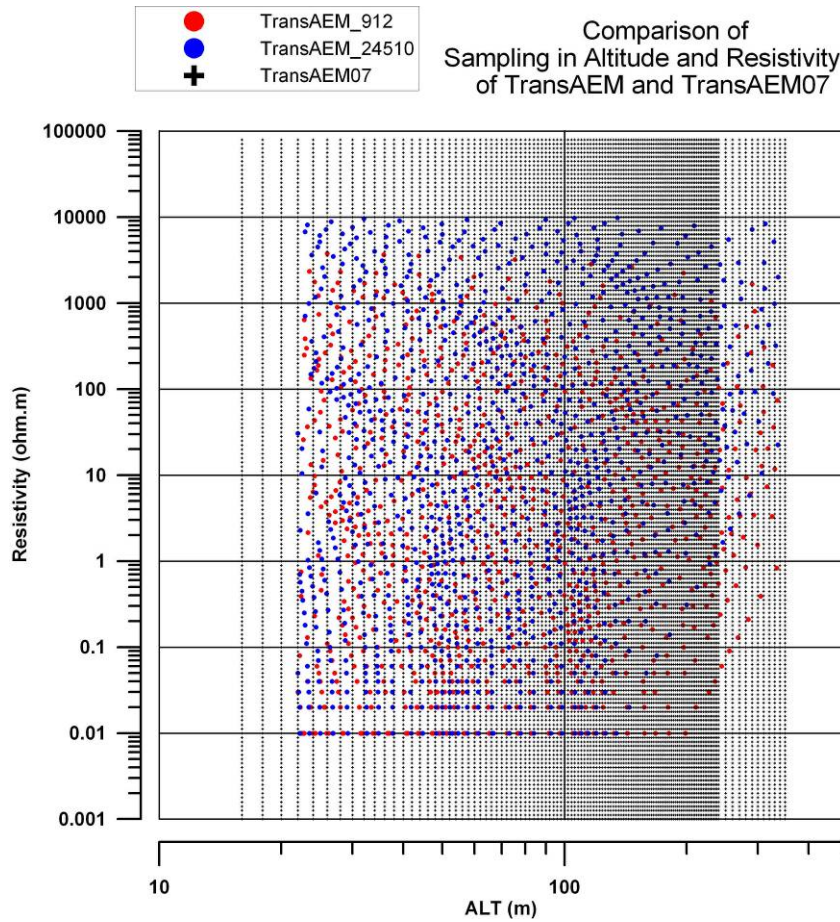


Figure A26. Comparison of sampling in altitude and resistivity of TransAEM and TransAEM07.

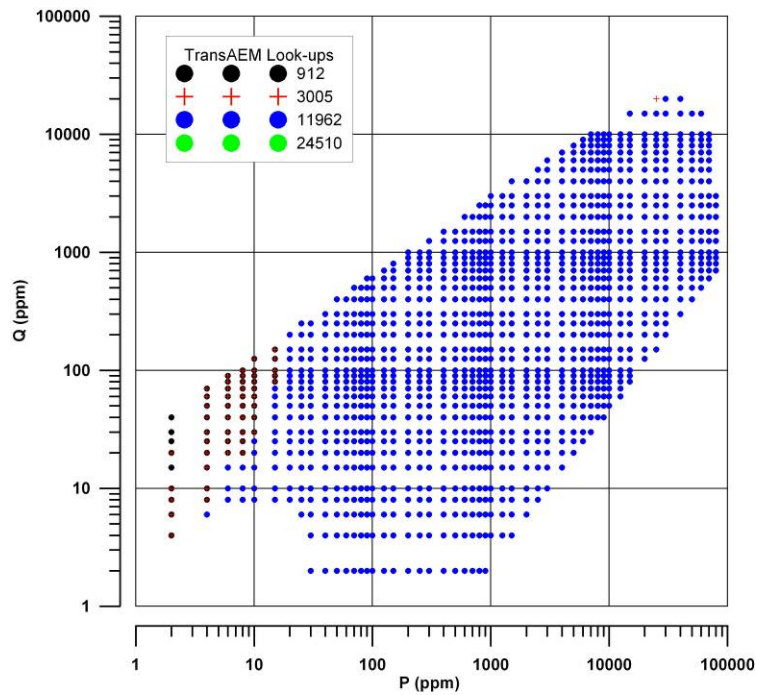
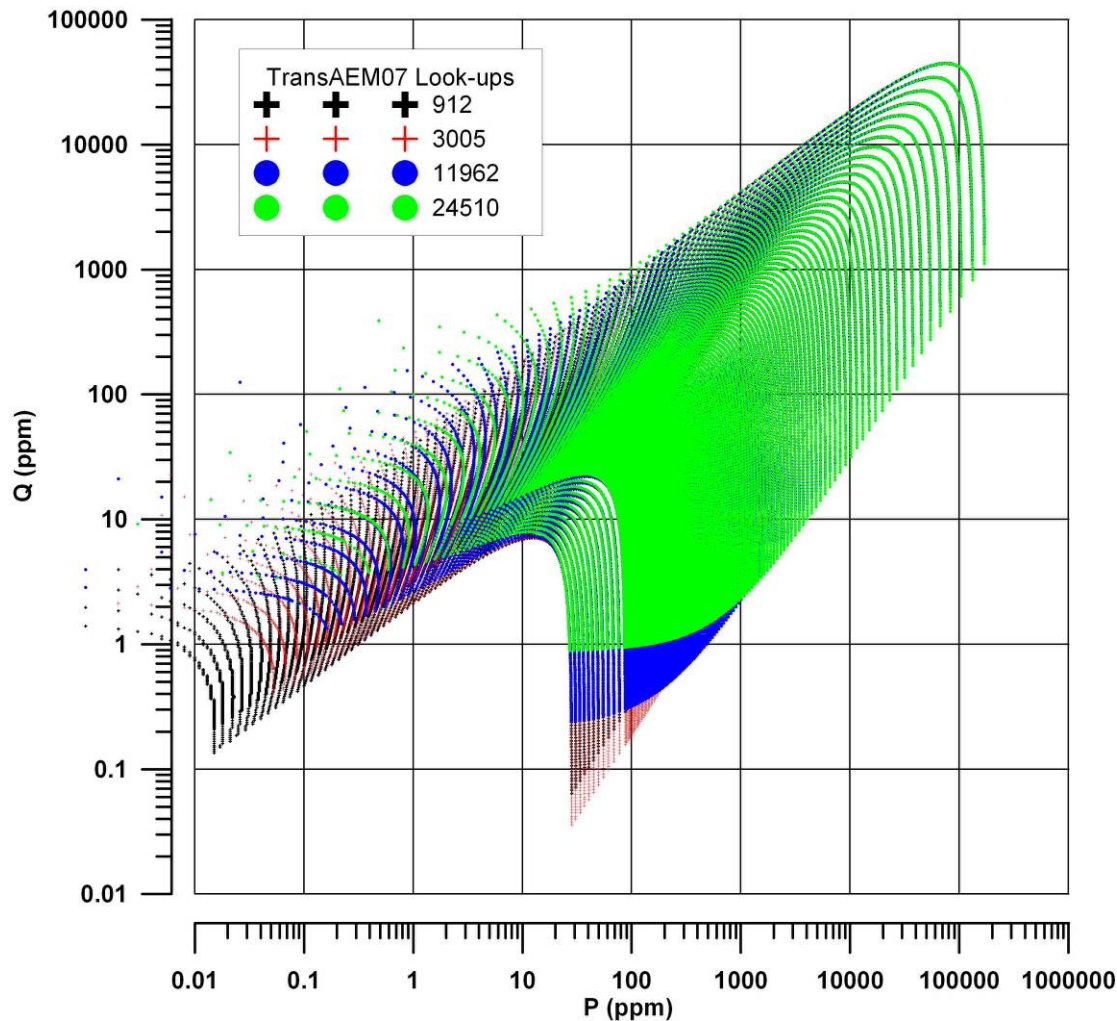


Figure A27. TransAEM nomograms (digital look-up tables).

The resulting files are named RI\_JAC\_00912\_2135.txt, RI\_JAC\_03005\_2135.txt, RI\_JAC\_11962\_2138.txt and RI\_JAC\_24510\_2138.txt. They are ASCII text files with 4

columns corresponding to P (ppm), Q(ppm), Half-space resistivity (ohm.m) and Altitude (m). The sampling in P&Q provided by the new nomograms is shown in Figure A28. The number of points used is 19716 and is the same for all 4 frequencies.



**Figure A28.** TransAEM07 nomograms (digital look-up tables).

Although in a practical sense, the range could be restricted to  $P, Q > 1$ , the complete data set is retained since it allows for regions where one of the components is  $> 1$  while its partner is  $< 1$ . The forward algorithm loses accuracy when values are  $\ll 1$  and scattering is observed in the nomograms at low P values (Q still valid).

### Notes on the low value P,Q thresholds

Low value thresholds were used in TRANSAEM, to limit negative and low amplitude data values in P,Q. They are used again here but the general subject is worth a bit of further discussion. Each threshold value is a clipping amplitude, such that all P or Q values less than this value (e.g.  $P_{\text{threshold}}$ ,  $Q_{\text{threshold}}$ ) are set to the value. The user is allowed to set different P,Q thresholds (e.g.  $P_{\text{threshold}} \neq Q_{\text{threshold}}$ ) but it is not recommended.

If values below the threshold were truly noise then we could/should(?) exclude them from the input file used by the program, or exclude them from the output file. We choose not to do this, because this would lead to ‘holes’ in the apparent resistivity/depth data sets. This might lead to

difficult data sets for both further levelling and gridding. We choose to fill the points where we cannot provide estimates.

Assuming we wish to set low value thresholds, and assume that  $P_{\text{threshold}} = Q_{\text{threshold}}$ . The value chosen will simply set the points with P,Q values below the threshold, to have a maximum AP and AD that is a function of frequency. The maximum values are tabulated in Table A3. A different table would have to be produced if we choose different threshold ratios of P,Q (i.e. other than unity).

**Table A3. Low value P,Q (P=Q) thresholds and resulting maximum AP, AD estimates**

P,Q ppm	Max Apparent resistivity (ohm.m)				Max Apparent Depth (m)			
	Frequency (Hz)				Frequency (Hz)			
	912	3005	11962	24510	912	3005	11962	24510
7.5	1633	5180	13897	17867	299	296	285	298
10	1331	4256	12025	15943	269	274	256	269
15	995	3213	9804	13473	228	234	222	229
20	797	2577	8460	11904	203	210	196	201
30	596	1949	6750	9942	173	175	165	170
40	487	1592	5714	8776	156	155	144	149
50	416	1365	4957	7972	145	139	129	132
70	325	1066	3987	6756	126	119	115	113
90	271	890	3364	5904	112	107	104	96
110	236	774	2957	5288	100	101	95	87
120	221	726	2784	5036	97	97	91	83

\*\*\* Note that threshold values of less than 7.5 produce unreliable results (with the present algorithm) and are not recommended.

The following comments are survey/data dependent. They would be different for a simple high-fly or a simple (i.e. small) low-fly survey. However, many surveys will contain a significant percentage of high-fly (low amplitude) data. Thus if we set P,Q to 20 ppm at all 4 frequencies, the resulting AP data and their ideal grids would have maximum AP values ranging from 797 ohm.m at 912 Hz to 11904 ohm.m at 24510 Hz. This can be viewed as something of a frequency-dependent distortion when there are substantial areas where the thresholds are applied. It may not be significant when the number of low P,Q values is small. The effect we see in the table (limited range of high resistivities at the two lowest frequencies) can be seen as a limited resistivity aperture across the four frequencies.

[An aside. What is happening is that the physics/maths for the no-magnetic-susceptibility model cannot provide low P,Q values at the 2 lowest frequencies. Looking at the knee of the nomogram

(Fig. A27), the low values for the two lowest frequencies are generated by the highest altitude portion of the nomogram ( $HT > 250$  m). This is in fact, a purely numerical trick to populate the nomogram (the AD values from these points would be noise). All-in-all, we have a limited high resistivity aperture, at low frequencies, because we don't take into account magnetic susceptibility.]

As well as the low value (threshold) issues discussed above, there is a further characteristic feature of our EM data sets. The nomograms occupy a region in P,Q space that DEFINE the region of validity of the apparent resistivity estimates calculated on the basis of:

- Uniform half-space (i.e. 1D) with fixed resistivity
- Relative magnetic permeability = 1, and ignoring dielectric effects (electrical permittivity).
- No other sources of EM (no power-line interference, etc)

Observed P,Q values that extend beyond the region defined by the nomograms may be generated by these additional influences.